Regulation of light harvesting in Chlamydomonas: two protein phosphatases are involved in state transitions

Federica Cariti[1], Marie Chazaux[2], Linnka Lefebvre-Legendre[1], Paolo Longoni[3], Bart Ghysels[2,4], Xenie Johnson[2], Michel Goldschmidt-Clermont[1,5]

[1]Department of Botany and Plant Biology, University of Geneva, 30 quai Ernest Ansermet, 1211, Genève 4, Switzerland

[2] Aix Marseille Univ., CEA, CNRS, BIAM, Saint Paul-Lez-Durance, France F-13108

[3] Current address : Université de Neuchâtel, 2000 Neuchâtel, Switzerland

[4] Current address : Université de Liège, Laboratoire de Bioénergétique, 4000 Liège, Belgium

[5] Institute of Genetics and Genomics of Geneva (iGE3), University of Geneva, Geneva, Switzerland

Author contributions:

MGC and XJ conceived and coordinated the research project, FC, MC, LLL, MGC, PL and BG performed the experiments and analyzed the data, MGC and FC wrote the article with contributions of all the authors, MGC agrees to serve as the author responsible for contact and ensures communication.

ABSTRACT

Protein phosphorylation plays important roles in short-term regulation of photosynthetic electron transfer. In a mechanism known as state transitions, the kinase STATE TRANSITION 7 (STT7) of *Chlamydomonas reinhardtii* phosphorylates components of light-harvesting antenna complex II (LHCII). This reversible phosphorylation governs the dynamic allocation of a part of LHCII to photosystem I or photosystem II, depending on light conditions and metabolic demands. Little is however known in the green alga on the counteracting phosphatase(s). In Arabidopsis, the homologous kinase STN7 is specifically antagonized by PROTEIN PHOSPHATASE 1/THYLAKOID-ASSOCIATED PHOSPHATASE 38 (PPH1/TAP38). Furthermore, the paralogous kinase STN8 and the countering phosphatase PHOTOSYSTEM II PHOSPHATASE (PBCP), which count subunits of PSII amongst their major targets, influence thylakoid architecture and high-light tolerance. Here we analyze state transitions in *C. reinhardtii* mutants of the two homologous phosphatases, CrPPH1 and CrPBCP. The transition from state 2 to state 1 is retarded in *pph1*, and surprisingly also in *pbcp*. However both mutants can eventually return to state 1. In contrast, the double mutant *pph1;pbcp* appears strongly locked in state 2. The complex phosphorylation patterns of the LHCII trimers and of the monomeric subunits are affected in the phosphatase mutants. Their analysis indicates that the two phosphatases have different yet overlapping sets of protein targets. The dual control of thylakoid protein de-phosphorylation and the more complex antenna phosphorylation patterns in Chlamydomonas compared to Arabidopsis are discussed in the context of the stronger amplitude of state transitions and the more diverse LHCII isoforms in the alga.

INTRODUCTION

To fulfill their energy requirements, photoautotrophic plants and algae rely on a photosynthetic electron transfer chain embedded in the thylakoid membrane of the chloroplast. Two photosystems (PSII and PSI) and their associated light-harvesting antennae (LHCII and LHCI) mediate the conversion of light energy into chemical energy. In the linear mode of electron flow (LEF), PSII and PSI work in series to extract electrons from water and to reduce ferredoxin (Fd) and NADPH. The two photosystems are connected through the plastoquinone pool, the cytochrome b_6f complex and plastocyanin. Electron transfer along the chain is coupled to proton accumulation in the luminal compartment of the thylakoid membranes, and the resulting proton gradient is used to drive ATP synthesis. In the cyclic mode of electron flow (CEF), which involves PSI and the cytochrome b_6f complex, ATP is produced but there is no net reduction of Fd and $NADP^+$. The chemical energy that is stored in ATP, reduced Fd and NADPH fuels cell metabolism, and in particular the synthesis of storage compounds such as carbohydrates. In the dark, in sink tissues or during the night, these compounds can in turn provide energy through glycolysis, respiration or fermentation.

While the photosystems are highly conserved in evolution, the light-harvesting antennae and their organization within the photosynthetic supercomplexes, are more diverse. In plants LHCI is constituted of four monomeric subunits (Lhca1-4) stably associated with PSI, while in *Chlamydomonas reinhardtii* (hereafter “Chlamydomonas”), LHCI is composed of ten subunits (two Lhca1 and one each of Lhca2 to Lhca9) (Takahashi et al., 2004; Drop et al., 2011; Mazor et al., 2015; Ozawa et al., 2018; Kubota-Kawai et al., 2019). In plants LHCII is composed of trimers containing combinations of Lhcb1, Lhcb2 and Lhcb3, and of monomeric subunits Lhcb4 (CP29), Lhcb5 (CP26) and Lhcb6 (CP24). In Chlamydomonas, the LHCII trimers are made of 8 different subunits encoded by 9 genes (LHCBM1-9, with LHCBM2 and LHCBM7 sharing an identical amino-acid sequence) while there are only 2 types of monomeric subunits, LHCB4 and LHCB5 ((Elrad and Grossman, 2004; Merchant et al., 2007); reviewed by (Minagawa and Takahashi, 2004; Crepin and Caffarri, 2018)).

Both external and internal factors induce responses that regulate the activity of the photosynthetic machinery (Eberhard et al., 2008). External conditions of temperature and light vary widely, over timescales that range from months for changes linked to the seasons, to minutes or seconds for those related to the weather or the patchy shade of a canopy. Rapid variations in light are challenging for photosynthetic organisms, which have to optimize light harvesting when photon flux is limiting, but avoid photo-damage when light is in excess. The internal demand for ATP or reducing power can also vary widely and rapidly

depending on metabolic activities, so that electron transport has to be adapted accordingly through regulatory responses of the photosynthetic machinery (Yamori and Shikanai, 2016).

Under limiting light, the mechanism of state transitions is an important regulator for the redox balance of the electron transport chain, through the reversible allocation of a part of LHCII to either PSII or PSI (Rochaix, 2014). In state 1 (St 1), this mobile part of the antenna is connected to PSII, while in state 2 (St 2) it is at least in part connected to PSI (Nagy et al., 2014; Unlu et al., 2014; Wlodarczyk et al., 2015; Nawrocki et al., 2016; Iwai et al., 2018). State transitions represent a negative feedback regulatory loop that is important to maintain the redox homeostasis of the plastoquinone (PQ) pool: reduction of the pool favors St 2 leading to an increase in the cross-section of the antenna connected to PSI, whose activity oxidizes the pool. Conversely, oxidation of the PQ pool favors St 1 leading to an increase in the cross-section of PSII, which promotes reduction of the pool. Under normal conditions, the system maintains an intermediate state between St 1 and St 2, which ensures a balanced ratio of reduced and oxidized PQ (Goldschmidt-Clermont and Bassi, 2015). In higher plants such as Arabidopsis, state transitions operate under low light in response to changes in light quality, for example under a canopy where the spectrum is enriched in far-red light, which is more efficiently absorbed by PSI than PSII. Thus, St 1 can be experimentally favored by illumination with far-red light, while St 2 is promoted by blue light. In Chlamydomonas, the difference in spectral properties of the two photosystems is not as pronounced (Tapie et al., 1984). However, a strong transition towards St 2 involving a large part of the LHCII antenna is promoted by anaerobiosis in the dark (Wollman and Delepelaire, 1984; Bulte and Wollman, 1990). For lack of oxygen, production of ATP by mitochondrial respiration is prevented, as well as PQH_2 oxidation by chloroplast PTOX (PLASTID TERMINAL OXIDASE), while fermentative metabolism produces an excess of reducing equivalents leading to a strong reduction of the PQ pool (Bulte et al., 1990; Houille-Vernes et al., 2011). CEF is tuned by redox conditions independently of state transitions (Takahashi et al., 2013). However, by favoring the activity of PSI, St 2 will enhance CEF and the production of ATP, at the expense of LEF and the production of reducing power which depend on PSII (Finazzi et al., 2002).

The transition towards St 2 is regulated through phosphorylation of LHCII by the protein kinase STN7 in higher plants (Bellafiore et al., 2005), or its orthologue STT7 in Chlamydomonas (Fleischmann et al., 1999; Depege et al., 2003; Lemeille et al., 2010). The activation of this kinase requires an interaction with the stromal side of the cytochrome b_6f complex and the docking of PQH_2 to the Q_o site of the complex (Vener et al., 1997; Zito et al., 1999; Dumas et al., 2017). The process is rapidly reversible, because the kinase is counteracted by the protein phosphatase PPH1/TAP38 in higher plants (Pribil et al., 2010;

115 Shapiguzov et al., 2010), which favors the transition towards St 1. In Arabidopsis the PSI-
116 LHCI-LHCII supercomplex, which is characteristic of St 2, contains one LHCII trimer which
117 belongs to a pool that would be loosely associated with PSII in St 1 (L trimers) (Galka et al.,
118 2012). This trimer contains both Lhcb1 and Lhcb2 subunits, but it is the phosphorylation of
119 the Lhcb2 isoform which is crucial for state transitions by favoring docking of the LHCII trimer
120 to PSI (Pietrzykowska et al., 2014; Crepin and Caffarri, 2015; Longoni et al., 2015; Pan et
121 al., 2018). Recently, PSI-LHCI-LHCII complexes with a second LHCII trimer have been
122 observed (Benson et al., 2015; Yadav et al., 2017). In Chlamydomonas, STT7
123 phosphorylates several subunits of LHCII trimers, and also the monomeric antenna LHCB4
124 (CP29) (Turkina et al., 2006; Lemeille et al., 2010). The other monomeric antenna, LHCB5
125 (CP26) can also be phosphorylated in this alga (Bassi and Wollman, 1991). In
126 Chlamydomonas, the PSI-LHCI-LHCII complex involves one or two LHCII trimers, and
127 strikingly also the monomeric antennae LHCB4 (CP29) and LHCB5 (CP26) (Takahashi et
128 al., 2006). The LHCBM5 isoform of LHCII was found to be particularly enriched in this
129 complex, but other LHCBM subunits appear to also participate in its formation and to be
130 phosphorylated (Drop et al., 2014). The LHCBM2/7 subunits stabilize the trimeric LHCII and
131 are also part of the PSI-LHCI-LHCII complex, although they may not be themselves
132 phosphorylated (Ferrante et al., 2012; Drop et al., 2014). It has been reported that
133 supercomplexes of PSI involving the cytochrome b_6f complex can be isolated from cells in St
134 2 or in anaerobic conditions (Iwai et al., 2010; Steinbeck et al., 2018). They are proposed to
135 facilitate CEF and thus favor the production of ATP. However the presence and significance
136 of these complexes is still a matter of debate (Buchert et al., 2018).

137 The protein kinase STN7 has a paralog called STN8 (Vainonen et al., 2005), which is
138 involved in the phosphorylation of numerous thylakoid proteins including the core subunits of
139 PSII (Reiland et al., 2011). The protein phosphatase PBCP is required for the efficient de-
140 phosphorylation of these subunits (Samol et al., 2012; Puthiyaveetil et al., 2014; Liu et al.,
141 2018). While there is some overlap in their substrate specificities, the antagonistic pairs of
142 kinases and phosphatases appear to have fairly distinct roles. STN7 and PPH1/TAP38 are
143 mainly involved in LHCII phosphorylation and state transitions, while STN8 and PBCP
144 influence the architecture of thylakoid membranes and the repair cycle of photo-inhibited
145 PSII. In monocots such as rice, a further role STN8 and PBCP in the high-light induced
146 phosphorylation of the monomeric LHCII subunit Lhcb4 (CP29) has been proposed (Betterle
147 et al., 2015; Betterle et al., 2017; Liu et al., 2018).

148 While the state-transition kinase STT7 was first identified in Chlamydomonas (Depege et al.
149 (2003), the functional homologs of the plant PPH1/TAP38 and PBCP phosphatases had not
150 been characterized yet in the alga. Here we present evidence that in Chlamydomonas,

151 homologs of PPH1/TAP38 and PBCP play a role in the regulation of state transitions, with
152 partially redundant functions.

153

RESULTS

CrPPH1 plays a role in state transitions

The closest homologue of the Arabidopsis gene encoding the thylakoid phosphatase PPH1/TAP38 (*At4G27800*) was identified in Chlamydomonas as *Cre04.g218150* in reciprocal BLASTP searches (see Materials and Methods) The Chlamydomonas protein, which we call CrPPH1, shares 36% sequence identity and 55% similarity with its *A. thaliana* homologue. In order to investigate the function of CrPPH1 in Chlamydomonas, we obtained a mutant strain from the CLiP library (LMJ.RY0402.16176, (Li et al., 2016)) with a predicted insertion in intron 7 of the *PPH1* gene (Fig. 1A). The site of insertion was confirmed by PCR amplification and sequencing of the amplified product (Fig. S1A). This mutant line showed an alteration of state transitions as will be detailed below. However, according to the CLiP database, this line also carried a second insertion (hereafter *ins2*) in gene *Cre24.g755597.t1.1*, an insertion that was similarly confirmed by PCR analysis (Fig. S1B). To remove the second mutation and to test whether the state transition phenotype co-segregated with the *pph1* mutation, the mutant line (*pph1;ins2*) was back-crossed twice to the parental strain CC5155 (Fig. S1C). From the first cross, 60 complete tetrads were analyzed for paromomycin resistance and for the presence of *pph1* and *ins2* insertions, both of which conferred paromomycin resistance. In 8 of these tetrads where the two insertions segregated (non-parental ditypes with four paromomycin-resistant colonies *pph1 / pph1 / ins2 / ins2*), we found that altered state transitions correlated with the insertion in the *pph1* gene (Fig. S1C). In a second backcross between a *pph1* single mutant deriving from the first backcross and the parental line CC5155, we analyzed 8 complete tetrads and observed co-segregation of the insertion in the *pph1* gene with paromomycin resistance and the state transition phenotype (Fig. S1D). This analysis shows that the alteration in state transitions is genetically tightly linked to the *pph1* mutation. To facilitate biochemical experiments, we further crossed a *pph1* mutant progeny to the cell-wall deficient strain *cw15*, and a double mutant, *pph1;cw15,* was selected for further analysis. All subsequent experiments were performed comparing the parental *cw15* strain with the double mutant *pph1;cw15*, however hereafter for simplicity these strains will be referred to as wild type (WT) and *pph1* respectively. The chlorophyll content and the maximum quantum efficiency of PSII were similar in *pph1* and in the wild type (Table S1). The *pph1* mutant also showed normal growth in a variety of conditions (Fig. S2).

A rabbit antiserum was raised against recombinant CrPPH1 expressed in *Escherichia coli* (Fig. S3A). It was used to assess the presence of the protein by immunoblotting of total protein extracts of the wild type and of the *pph1* mutant (Fig. 1B). A band was observed in

the wild type that was not detected in the *pph1* mutant. This band migrated with an apparent molecular mass of 45 kDa, somewhat slower compared to the calculated 40 kDa molecular mass of CrPPH1 after removal of a predicted chloroplast transit peptide of 52 to 56 amino acid residues according to different algorithms (Predalgo, (Tardif et al., 2012), ChloroP (Emanuelsson et al., 1999)). Because of the background signal with this antibody, a low level of residual CrPPH1 expression in the *pph1* mutant could not be excluded (Fig. S3).

State transitions can be monitored as a change in the fluorescence emission spectrum at 77 K (Fig. 1C). In Chlamydomonas, the transitions can be experimentally induced by switching between anaerobic and aerobic conditions. In the dark, anaerobiosis leads to reduction of the PQ pool and consequent establishment of State 2 (St 2). Subsequent strong aeration under the light promotes oxidation of the PQ pool and a transition to St 1. The relative sizes of the peaks at 682 nm and 712 nm qualitatively reflect changes in the light harvesting antennae associated with PSII and PSI respectively. In the wild type, transition from St 2 (LHCII partly connected to PSI) to St 1 (LHCII mostly allocated to PSII) caused a decrease in the PSI peak relative to the PSII peak. The spectrum was recorded after 20 minutes in the conditions promoting St 1, a timepoint when the transition is nearing completion in the wild type. At this time, the extent of the transition from St 2 towards St 1 was strongly diminished in the *pph1* mutant compared to the wild type (Fig. 1C).

The time courses of state transitions were analyzed in more detail by measuring room temperature Chl fluorescence using Pulse-Amplitude-Modulation (PAM) spectroscopy (Fig. 1D). Cells that had been acclimated to minimal medium in low light (60 µmol photons m^{-2} s^{-1}) were transferred to the PAM fluorometer and the sample chamber was sealed, so that consumption of oxygen by respiration led to anaerobiosis. Steady state fluorescence (F_s) was continuously monitored with the low-intensity measuring beam to monitor the redox state of the PQ pool, and saturating flashes were applied every 4 minutes to measure the maximum fluorescence of PSII (F_m'), which correlates with the cross-section of its functional light-harvesting antenna. Reduction of the PQ pool in the dark (denoted by an increase in F_s) triggered the transition to St 2 in the wild type and the *pph1* mutant (decrease of F_m'). The chamber was then opened and the algal sample bubbled with air, restoring an aerobic environment and allowing the re-oxidation of the PQ pool and a transition towards St 1 (increase of F_m'). We observed that the transition from St 2 to St 1 was strongly delayed in *pph1* (Fig. 1D), consistent with a role of CrPPH1 in de-phosphorylation of the LHCII antenna. A role in state transitions was confirmed using another protocol (Hodges and Barber, 1983; Wollman and Delepelaire, 1984), whereby the transition from St 2 to St 1 was induced by actinic light in the presence of the PSII inhibitor DCMU (3-(3,4-dichlorophenyl)-1,1-dimethylurea) under continued anaerobiosis (Fig. S4). The fact that at the onset of these

experiments, *pph1* is capable of a transition from St 1 towards St 2 implies that although the subsequent transition towards St 1 is delayed, *pph1* can eventually reach at least a partial St 1 under the culture conditions used prior to the measurements (Fig. 1C, D and Fig. S4).

To confirm that this state-transition phenotype is due to the *pph1* mutation, we transformed the mutant strain with a plasmid carrying a wild-type copy of *PPH1* in which we inserted a sequence encoding a triple HA (haemagglutinin) epitope at the 3' end of the coding sequence (*PPH1-HA*) and a selection marker (*aph7"*, hygromycin resistance). The transformants were screened by chlorophyll fluorescence spectroscopy, and 4 lines showing a restoration of state transitions were selected for further analysis. Immunoblotting with a monoclonal HA antibody indicated that the rescued lines (*pph1:PPH1-HA*) expressed the tagged CrPPH1-HA protein, and immunoblotting with the anti-CrPPH1 antibodies showed that the protein was expressed at levels similar to those of the wild type or in moderate excess (Fig. 2A). PAM fluorescence spectroscopy showed that in *pph1:PPH1-HA* the rate of the transition from St 2 to St 1 was comparable to that of the wild type (Fig. 2B).

To further test the role of CrPPH1 in LHCII de-phosphorylation, we examined the phosphorylation status of the major thylakoid proteins by SDS-PAGE and immunoblotting. St 2 was established by anaerobiosis in the dark, and a subsequent transition to St 1 was promoted by strong aeration in the light, as above for the analysis of fluorescence at 77 K. An antibody against phospho-threonine (P-Thr) revealed a complex pattern of phosphoproteins, nevertheless a distinct decrease in the signal of several bands was observed in the wild type upon transition from St 2 to St 1 (Fig. 1E), as well as in the complemented strains (Fig. 2C). As will be shown below, some of the same bands were clearly under-phosphorylated in the mutant *stt7*, which is deficient for the protein kinase involved in state transitions. In the *pph1* mutant, the signal of these phosphoprotein bands decreased much less after switching to the conditions that favor St 1. With an antibody against the phosphorylated form of Arabidopsis Lhcb2 (P-Lhcb2), several bands were observed in Chlamydomonas, corresponding to the migration of LHCII (Fig. S5), although the sequence divergence between the peptide recognized by the antibody and the potential target sequences in the Chlamydomonas antenna subunits does not allow a simple assignment to specific LHCBM isoforms. In the wild type, the intensity of these bands was higher in St 2 than St 1. In the *stt7* mutant (see below) these bands are detected only at low levels that are similar under St 2 or St 1 conditions. These two observations indicate that at least some of the bands revealed in Chlamydomonas by the Arabidopsis anti-P-Lhcb2 antibody are implicated in state transitions. These bands were clearly over-phosphorylated in *pph1* compared to the wild type in the conditions that favor a transition to St 1. Thus, the

alteration in state transitions observed spectroscopically in the *pph1* mutant correlates with defects in the de-phosphorylation of LHCII antenna components.

CrPBCP is also involved in state transitions

A striking feature of the *pph1* mutant was that it showed strong retardation of the transition from St 2 to St 1, but that nevertheless under normal culture conditions it was capable of approaching St 1 and undergoing a subsequent transition to St 2 (Fig. 1D and Fig. S4). It thus appeared that at least one other protein phosphatase might be involved in state transitions and de-phosphorylation of LHCII components, allowing the establishment of St 1 in *pph1*, albeit more slowly. This was corroborated by the identification of another phosphatase mutant affected in state transitions.

A library of mutants with random insertions of an *aphVIII* cassette (paromomycin resistance) was generated and screened using a fluorescence imaging set-up (Tolleter et al., 2011). To search for mutants in photoprotective or alternative electron transfer pathways this library was recently screened again using a different imaging system (Johnson et al., 2009). One of the mutants (identified as *pbcp*, see below) showed impaired transitions from St 2 to St 1 (Fig. 3). Using reverse-PCR techniques, the insertion was mapped to the gene *Cre06.g257850* (Fig. S6A), which encodes the closest homologue in Chlamydomonas of PBCP from Arabidopsis, and will be called CrPBCP hereafter (Fig. 3A). To test whether the alteration of state transitions was genetically linked to the *pbcp* mutation, we backcrossed the mutant to wild type 137C. In 40 complete tetrads, paromomycin resistance segregated with the insertion in the *PBCP* gene. In the 4 tetrads that we analyzed further, an over-phosphorylation of thylakoid proteins co-segregated with the insertion in *PBCP* (Fig. S6B). Moreover, *pbcp* and the phosphorylation phenotype also co-segregated with mating type minus (mt-), as expected because *PBCP* lies in close proximity to the mating-type locus on chromosome 6. One of the *pbcp* mutant progeny was further crossed to *cw15* to obtain a cell-wall deficient strain (*pbcp;cw15*) which was used in all subsequent experiments and will be referred to as *pbcp* hereafter. Using a rabbit antiserum raised against recombinant CrPBCP expressed in *E. coli* (Fig. S3B) and immunoblotting of total proteins separated by SDS PAGE, the protein was detected in the wild type but not in the *pbcp* mutant (Fig. 3B). The chlorophyll content and the maximum quantum yield of PSII were not significantly different in *pbcp* and in the wild type (Table S1). Furthermore, the *pbcp* mutant showed normal growth under a variety of conditions (Fig. S2).

293 We analyzed state transitions in the *pbcp* mutant by determining its fluorescence emission
294 spectra at 77 K in St 2 and after a subsequent transition to conditions promoting St 1 for 20
295 minutes. Compared to the wild type, the transition to St 1 was significantly impaired in *pbcp*
296 (Fig. 3C). Using PAM chlorophyll fluorescence spectroscopy, we observed that anaerobiosis
297 in the dark promoted a transition to St 2 in the *pbcp* mutant as in the wild type. However,
298 upon aeration and re-oxidation of the PQ pool, the transition from St 2 to St 1 was strongly
299 delayed in *pbcp* (Fig. 3D). Similar observations were made using the protocol where this
300 transition was induced by light in the presence of DCMU (Fig. S4). Thus, CrPBCP seems to
301 play a major role in state transitions, unlike its homologue in Arabidopsis.

302 To confirm that the state transition phenotype was due to the *pbcp* mutation, we transformed
303 the *pbcp* mutant with a plasmid carrying a wild-type copy of *PBCP* tagged with a sequence
304 encoding a triple HA epitope (*PBCP-HA*) and a selectable marker (*aph7''*). Four rescued
305 lines (*pbcp;PBCP-HA*) that expressed the tagged CrPBCP-HA protein were retained for
306 further analysis. Immunoblotting with the anti-PBCP antibodies (Fig. 4A) showed that the
307 different *pbcp;PBCP-HA* lines expressed the protein at levels similar or somewhat reduced
308 compared to the wild type. State transitions were restored in the *pbcp;PBCP-HA* lines, as
309 monitored by PAM fluorescence spectroscopy (Fig. 4B).

310 To investigate the alteration of thylakoid protein phosphorylation in the *pbcp* mutant, we
311 used SDS-PAGE and immunoblotting (Fig. 3E). With an anti-P-Thr antibody we observed
312 that bands which migrate as components of LHCII (Fig. S5) were over-phosphorylated in
313 *pbcp*, but not in the complemented *pbcp;PBCP-HA* lines. Unfortunately, these commercial
314 anti-P-Thr antibodies (now discontinued) did not clearly identify the phosphorylated forms of
315 PSII subunits D2 (PsbD) or CP43 (PsbC) (Fig. S5). High phosphorylation of LHCII
316 constituents was confirmed with the Arabidopsis anti-P-Lhcb2 antibodies, which showed
317 over-phosphorylation in *pbcp* of the bands that are under-phosphorylated in the *stt7* mutant.
318 Thus, CrPBCP has a different range of targets in Chlamydomonas than its homologue in
319 Arabidopsis, where the major targets of PBCP are the subunits of the PSII core. It was
320 striking that excess phosphorylation of thylakoid proteins in *pbcp* appeared not only after a
321 transition from St 2 to St 1, but also under normal growth conditions (GL, 80 µmol photons
322 m^{-2} s^{-1}), as well as after growth under high light (HL, 300 µmol photons m^{-2} s^{-1}) or in the dark
323 (Fig. 3F).

324

325 **The *pph1;pbcp* double mutant is locked in state 2**

326 Both CrPPH1 and CrPBCP are implicated in the de-phosphorylation of some components of
327 LHCII and are essential for an efficient transition from St 2 to St 1. Nevertheless, both

individual mutants, *pph1* and *pbcp*, are capable of eventually approaching St 1 under the culture conditions prior to the measurements (Figs. 1D, 3D and S4). To further test whether the two phosphatases play partly redundant roles in the regulation of state transitions, we generated double *pph1*;*pbcp* mutants by crossing *pph1* and *pbcp* and genotyping the progeny by PCR (Fig. S7). The *pph1;pbcp* mutants also carry the *cw15* mutation like both their parents. The double mutants were, as expected, deficient for both CrPPH1 and CrPBCP (Fig. 5A). The maximum quantum yield of PSII and the chlorophyll content of *pph1;pbcp* were not significantly different from the wild type (Table S1), and the double mutant showed normal growth under a set of different conditions that were tested (Fig. S2).

When state transitions were monitored in *pph1*;*pbcp* double mutants, it was remarkable that, following pre-acclimation under low light where the wild-type cells are in St 1, the double mutant had a comparatively low value of F_m' at the onset of the measurements, indicative of St 2 (Fig. 5B). There was also no significant further drop in F_m' when the *pph1;pbcp* sample became anaerobic with the concomitant rise in F_s. The double mutant also showed no rise in F_m' when the sample was aerated again, indicating that the transition to St 1 was severely hampered. Similar results were obtained when this state transition was promoted by light in the presence of DCMU (Fig. S4). The low level of F_m' indicative of St 2 correlated with a high phosphorylation of LHCII components (Fig. 5C). In contrast to the wild type which showed low phosphorylation in St 1, high phosphorylation after a transition to St 2, and again low phosphorylation after a further transition to St 1, *pph1;pbcp* showed in all three conditions a phosphorylation pattern similar to that of the wild type in St 2 (Fig. 5C). These observations indicated that the *pph1;pbcp* double mutant is essentially locked in St 2. In further support of this conclusion, we determined the fluorescence emission spectrum at 77 K of cells in all three conditions (St 1 > St 2 > St 1), and observed that in the *pph1;pbcp* double mutant the fluorescence emission peak of PSI relative to PSII was always larger than in the wild type (Fig. 5 D and Fig. S4B). Our data indicate that two partially redundant protein phosphatases, CrPPH1 and CrPBCP, are involved in the transition from St 2 to St 1.

Accumulation of thylakoid proteins in the mutants

In Arabidopsis, the expression of STN7 is reduced under prolonged exposure to far-red light (Willig et al., 2011), and the amount of PPH1 is down-regulated at a post-transcriptional level in the *psal* mutant, which is deficient in the docking of LHCII to PSI and thus incapable of completing state transitions (Rantala et al., 2016). These observations prompted us to determine whether in Chlamydomonas the amounts of STT7, CrPPH1 or CrPBCP are altered in the single kinase or phosphatase mutants as well as in the *pph1;pbcp* double

363 mutant, using SDS PAGE and immunoblotting of protein extracts from cells grown under
364 normal conditions (Fig. 5A). However, no significant differences were observed in the
365 accumulation of the three regulatory proteins.

366 We also investigated the possibility that the phosphatase mutations might be compensated
367 in the long term by changes in the stoichiometry of the photosystems or other major
368 photosynthetic complexes. Proteins extracts of the wild type, the single mutants *pph1* and
369 *pbcp* as well as the double mutant *pph1;pbcp* grown under normal conditions were
370 compared by SDS PAGE and immunoblotting (Fig. S8). Antisera against representative
371 subunits of the major complexes were used for this analysis: AtpB (ATP synthase), D1
372 (PSII), PsaA (PSI), Cytf (cytochrome b_6f complex) or COXIIb (mitochondrial cytochrome
373 oxidase). However, no significant differences were apparent in the relative amounts of the
374 photosynthetic complexes in the mutant lines.

375

376 **CrPPH1 and CrPBCP have overlapping but distinct de-phosphorylation targets**

377 In Chlamydomonas, LHCII is composed of monomeric LHCB4 (CP29) and LHCB5 (CP26)
378 as well as trimers of isoforms LHCBM1 through LHCBM9. Based on their primary
379 sequences, the trimer subunits belong to four types (Fig. S9): type I in which three
380 subgroups can be distinguished (LHCBM3; LHCBM4/LHCBM6/LHCBM8; LHCBM9), type II
381 (LHCBM5), type III (LHCBM2/LHCBM7, which are identical in mature sequence) and type IV
382 (LHCBM1). While the P-Thr antiserum and the Arabidopsis P-Lhcb2 antiserum showed clear
383 differences in the patterns of LHCII phosphorylation in St 1 in both phosphatase mutants
384 (Fig. 6A), the ill-defined specificity of these antisera did not allow the discrimination of the
385 different components of the antenna, or reveal any target specificity of the respective
386 phosphatases. To address these questions, we used Phos-tag polyacrylamide gel
387 electrophoresis (Phos-tag PAGE) followed by immunoblotting with specific antibodies. We
388 obtained previously described antisera against LHCB4, LHCB5 and LHCBM5 (type II)
389 (Takahashi et al., 2006), and also generated antisera against peptides that are characteristic
390 for the other types of LHCBM subunits. Because these isoforms share a high degree of
391 sequence similarity, the antigenic peptides were selected in the N-terminal region of the
392 proteins, which is the most divergent between LHCII types (Fig. S9). The specificity of the
393 affinity-purified antibodies was tested against the recombinant LHCII subunits expressed in
394 *E. coli* (Fig. S10). The antisera against LHCBM1 (type IV), LHCBM3 (type I), LHCB4 and
395 LHCB5 (minor antenna) proved to be very specific. The antiserum against LHCBM2/7 (type
396 III) showed minor cross-reactions towards type I isoforms. Finally the antiserum against
397 LHCBM4/6/8 (type I, which share the same sequence in the N-terminal region) also reacted

towards LHCBM3 (also type I) but unexpectedly very strongly decorated LHCBM9 (type I). It should be noted however, that LHCBM9 is only expressed under conditions of nutrient stress (Grewe et al., 2014).

To analyze the phosphorylation of the different proteins by immunoblotting, we used Phos-tag which is a metal chelator that can be cross-linked into a polyacrylamide gel during polymerization (Kinoshita et al., 2009). This chelator binds Zn^{2+} ions that interact with phosphate groups and thus retard the migration of phosphorylated forms of proteins during SDS-PAGE. After immunoblotting (Fig. 6B), the degree of phosphorylation of the target protein is reflected in the ratio of the bands representing one or more slower-migrating phospho-form(s) (labelled P) to the band corresponding to the faster-migrating non-phosphorylated protein (labelled NP). To determine the migration of the non-phosphorylated form, we treated a sample of the wild type in St 2 with a non-specific protein phosphatase (λ phosphatase) prior to electrophoresis (lane marked λ in Fig. 6B).The anti-peptide antibodies are targeted to the N-terminus of the LHCBM subunits, which also contains the major sites of phosphorylation. To avoid any bias due to differential recognition by these antibodies of the phosphorylated and non-phosphorylated forms of their targets, we treated the proteins after blotting onto the membrane with λ phosphatase (Longoni et al., 2015). Because the phosphatases play a role in the transition from St 2 to St 1, we analyzed protein extracts of the wild type and the different mutants in St 2 (induced by anaerobiosis in the dark) and after a subsequent transition to St 1 (triggered by aerating the sample).

The antibodies against LHCBM1 (type IV) labelled two bands in the wild type in St 2 (Fig. 6B). The lower one co-migrated with the single band in the λ-phosphatase-treated sample, representing the non-phosphorylated protein. The upper band, corresponding to a phosphorylated form, gave a strong signal relative to the lower one, indicative of a high degree of LHCBM1 phosphorylation in St 2. The ratio of the phosphorylated band to the non-phosphorylated one was much lower in the kinase mutant *stt7*, or after the transition to St 1. In the *pph1* mutant, strong phosphorylation of LHCBM1 was still apparent in the conditions promoting St 1, with a high ratio of the upper to the lower band, in contrast to the wild type or the *pbcp* mutant. The double mutant *pph1;pbcp* showed the same high degree of phosphorylation after the transition to St 1 conditions as the *pph1* mutant. We infer that CrPPH1 is a major actor of LHCBM1 de-phosphorylation during the transition to St 1.

The antibodies against LHCBM3 (type I) decorated two bands after Phos-tag gel electrophoresis of the λ-phosphatase-treated sample (Fig. 6B), as well as after conventional gel electrophoresis of an untreated sample (Fig. S8B), even though these antibodies were specific for LHCBM3 amongst the recombinant proteins expressed in *E. coli* (Fig. S10). The

lower band (marked with an asterisk), which was partially resolved as a doublet, is unlikely to represent processed forms of LHCBM3 lacking amino-acid residues at the N-terminus (Stauber et al., 2003) since the LHCBM3 antibodies were raised against this region and would not recognize a truncated protein. Thus the lower band may reflect non-specific binding to another protein. There were two additional slower-migrating bands in the wild type in St 2, largely absent from the λ-phosphatase-treated sample, suggesting that LHCBM3 may undergo phosphorylation at more than one site, or that the non-specific protein is phosphorylated as well. One of these bands were also clearly present in *stt7*, suggesting the involvement of another protein kinase in LHCBM3 phosphorylation. The relative intensity of the top-most of the phosphorylated bands to the non-phosphorylated ones clearly decreased after transition to St 1 in the wild type. Some de-phosphorylation was still apparent in the *pph1* mutant, but the overall phosphorylation level appeared to be higher. In contrast, the *pbcp* mutant showed a much higher ratio of phosphorylated bands in both St 2 and St 1, as did the *pph1;pbcp* double mutant. Thus, CrPBCP appears to play the major role for de-phosphorylation of LHCBM3.

With the antibodies against LHCBM4/6/8 (type I), a single major band was observed in the λ-phosphatase-treated sample (Fig. 6B), as well as after conventional gel electrophoresis (Fig. S8B). However, these antibodies also recognized other recombinant type I isoforms, LHCBM3 and LHCBM9 (Fig. S10). The latter should not be expressed under our conditions, since it is induced by nutrient stress (Grewe et al., 2014). After Phos-tag electrophoresis of the wild type sample in St 2, the pattern of phosphorylation was complex, with most bands corresponding to those revealed with anti-LHCBM3 (but excluding the band marked with an asterisk). One of the phosphorylated forms was present in the *stt7* mutant. The degree of phosphorylation of the others decreased in St 1 in both the wild type and *pph1*, but not in *pbcp* or *pph1;pbcp* where the most phosphorylated form was prevalent. We tentatively infer that CrPBCP is involved in de-phosphorylation of LHCBM4/6/8 and, since it also affects LHCBM3, more generally in the de-phosphorylation of type I isoforms.

The antibodies against LHCBM2/7 (type III) decorated a strong band in the λ-phosphatase-treated sample, with a second minor band above it. Likewise, after conventional gel electrophoresis, these antibodies labelled a major and a minor band (Fig. S8B). Amongst the recombinant proteins expressed in *E. coli*, the LHCBM2/7 antibodies strongly recognized LHCBM2/7, but also weakly cross-reacted with the type I isoforms LHCBM3, LHCBM4/6/8 and LHCBM9 (Fig. S10). The patterns of the phosphorylated bands together with the upper non-phosphorylated band (marked with a triangle), but excluding the strong non-phosphorylated band below (marked with a square), were similar to the pattern obtained with anti-LHCBM4/6/8, and may mostly represent the cross-reaction to these isoforms.

Compared to LHCBM4/6/8, the strong additional non-phosphorylated band (marked with a square) can tentatively be ascribed to LHCBM2/7, which is thus apparently not subject to phosphorylation under these conditions, or only to a small degree.

With antiserum against LHCBM5 (type II), two bands were detected in the λ-phosphatase-treated sample, and at least five more in the various genotypes in St 2. Two bands were also observed after conventional SDS-PAGE (Fig. S8B), which could represent processed forms of LHCBM5 or cross-reactions to other isoforms, so it is unclear which of the five upper bands correspond to phosphorylated LHCBM5. The four uppermost bands were missing in *stt7* suggesting that their phosphorylation relates to state-transitions. In the wild type in St 1 and in *stt7*, an additional band was present between the two non-phosphorylated ones, likely representing a low-phosphorylation form. Higher ratios of the upper bands to the lower ones were observed in St 1 in *pph1* and *pbcp*, and an even higher ratio in *pph1;pbcp*. These observations suggest that both CrPPH1 and CrPBCP act in a partly redundant manner on the phosphorylation of LHCBM5, and potentially other cross-reacting proteins decorated by the antibody.

Antiserum against LHCB4, which recognized a single band after conventional SDS-PAGE (Fig. S8B), decorated multiple bands in the wild-type in St 2, in accordance with the multiple phosphorylation sites that have been observed in LHCB4 (Lemeille et al., 2010). The upper bands were missing in *stt7*, and the ratio of the upper ones to the lower ones decreased in the wild type in St 1 compared to St 2. In *pph1*, the pattern in St 1 resembled that of St 2, while in *pbcp*, as well as in *pph1;pbcp*, a very high degree of phosphorylation was observed in both states. These data suggest that CrPPH1 and CrPBCP contribute to LHCB4 de-phosphorylation in St 1, and that CrPBCP may play such a role also in St 2, independently of state transitions.

The antiserum against LHCB5, which labels a single band after conventional SDS-PAGE (Fig. S8B), decorated at least three bands in the different samples, none of which co-migrated with the non-phosphorylated form in the λ-phosphatase-treated sample. Two of the constitutively phosphorylated forms were present in *stt7*, while the third and slowest-migrating form was present in the wild type in St 2 but not in St 1. The latter was still present in *pph1* in St 1, while it became prevalent compared to the lowest one in *pbcp*, and in *pph1;pbcp*. These observations suggest that CrPPH1 and CrPBCP participate in LHCB5 de-phosphorylation in St 1, and that CrPBCP may also contribute in St 2.

With antiserum against the PsbH subunit of PSII, two phosphorylated forms were observed in the wild type and in *stt7*, in both St 2 and St 1 conditions (Fig. 6B). Phosphorylation appeared stronger in *pbcp* as well as *pph1;pbcp*, suggesting that CrPBCP is probably

504 involved in the de-phosphorylation of PsbH, like its homologue in Arabidopsis (Samol et al.,
505 2012).

506 Finally with antiserum against PETO, which is a phospho-protein implicated in the regulation
507 of CEF (Hamel et al., 2000; Takahashi et al., 2016), a major phosphorylated form as well as
508 one or two minor ones were observed in the wild type in St 2, that were strongly diminished
509 in St 1 or in the *stt7* mutant. In *pph1* the phosphorylation was retained in St 1, in *pbcp* the
510 upper band became most prevalent, and in *pph1;pbcp*, an even slower-migrating band was
511 apparent. These data indicate that both CrPPH1 and CrPBCP are involved in the de-
512 phosphorylation of PETO in a somewhat additive manner.

513

514

515 **DISCUSSION**

516 We have identified two protein phosphatases that are required for efficient transitions from St
517 2 to St 1 in Chlamydomonas. CrPPH1 is the closest homolog of Arabidopsis PPH1/TAP38,
518 which is involved in state transitions in the plant (Pribil et al., 2010; Shapiguzov et al., 2010).
519 Unexpectedly, we found that in Chlamydomonas CrPBCP is also involved in state
520 transitions. This is in contrast to PBCP from Arabidopsis, which is required for the de-
521 phosphorylation of several PSII core subunits but not of the LHCII antenna (Samol et al.,
522 2012). In Arabidopsis, lack of PBCP does not affect state transitions and it is only when this
523 phosphatase is strongly over-expressed that it has a minor effect on the rate of state
524 transitions. In rice, OsPBCP contributes to de-phosphorylation of LHCB4 (CP29), and is
525 proposed to have a role in regulating the dissipation of excess energy (Betterle et al., 2017).
526 The different substrate specificities of the two phosphatases from higher plants can be
527 explained by the different geometry of their substrate binding sites (Wei et al., 2015; Liu et
528 al., 2018).

529 The transition from St 2 to St 1 is strongly delayed in the *pph1* and *pbcp* mutants of
530 Chlamydomonas. However after incubation in conditions favoring St 1, both single mutants
531 are nevertheless capable of approaching St 1 (Figs. 1D, 3D and S4), and then to undergo a
532 transition towards St 2. In contrast, the double mutant *pph1;pbcp* remains in St 2 even in the
533 conditions that favor St 1 in the wild type (Figs. 5 and S4). Thus the phenotypes of the two
534 mutants show some additivity, but the two phosphatases have partly redundant functions in
535 state transitions.

536 State transitions are regulated by the phosphorylation or de-phosphorylation of LHCII
537 antenna proteins. In Arabidopsis, the Lhcb1 and Lhcb2 components of the LHCII trimers can
538 be phosphorylated, but not Lhcb3, with phospho-Lhcb2 playing a major role in the formation
539 of the PSI-LHCI-LHCII complexes in St 2 (Crepin and Caffarri, 2015; Longoni et al., 2015).
540 To investigate the requirement of CrPPH1 and CrPBCP in antenna de-phosphorylation
541 during a transition from St 2 to St 1 in Chlamydomonas, we used Phos-tag PAGE and
542 immunoblotting (Fig. 6B). Although some of the anti-peptide antisera that we developed
543 displayed some cross-reactions amongst closely related LHCBM isoforms, it was still
544 possible to assign many phosphorylated forms to the different types of LHCBM. The Phos-
545 tag PAGE technique has the advantage of allowing an assessment of cumulative
546 phosphorylation. Compared to the simple patterns that are obtained with Lhcb1 and Lhcb2 in
547 Arabidopsis (Longoni et al., 2015), which each one having only a single major
548 phosphorylated form, the patterns proved much more complex in Chlamydomonas, raising
549 the possibility that some LHCBM isoforms may undergo multiple phosphorylation. The

550 analysis revealed interesting differences and overlaps between the targets of CrPPH1 and
551 CrPBCP. CrPPH1 was essential for de-phosphorylation of the type IV isoform LHCBM1,
552 while mainly CrPBCP was required for de-phosphorylation of the type I isoforms LHCBM3
553 and LHCBM4/6/8. Both CrPPH1 and CrPBCP were necessary for de-phosphorylation of the
554 type II isoform LHCBM5 as well as the minor antennae LHCB4 and LHCB5, with CrPBCP
555 playing a dominant role for LHCB4. An over-phosphorylation phenotype was already
556 apparent in St 2 in the *pbcp* mutant for LHCBM3, LHCB4 and LHCB5 and, although to a
557 lower extent, LHCBM3 and LHCBM5 appeared over-phosphorylated in *pph1* under St 2
558 conditions. After growth under constant condition of low light or high light, over-
559 phosphorylation was also observed in the *pbcp* mutant by immunoblotting with anti-P-Thr
560 antibodies. It thus appears that CrPBCP may be active in de-phosphorylation status of
561 thylakoid proteins not only in conditions that promote St 1, but also under more balanced
562 steady-state conditions.

563 In Arabidopsis, PPH1 is specific for LHCII, although its strong over-expression has an effect
564 on the de-phosphorylation of the PSII core subunits D1 and D2 (Pribil et al., 2010;
565 Shapiguzov et al., 2010). Conversely, PBCP is mostly required for dephosphorylation of PSII
566 subunits (D1, D2 and CP43), but it can also act on LHCII (Samol et al., 2012; Longoni et al.,
567 2019). In Chlamydomonas the major phosphorylated thylakoid proteins include, in addition to
568 LHCII, some subunits of PSII (D2 (PsbD), CP43 (PsbC) and PsbH) (Delepelaire, 1984; de
569 Vitry et al., 1991) as well as PETO (Hamel et al., 2000). Using Phos-tag gel electrophoresis,
570 we found that both CrPPH1 and CrPBCP influence not only the de-phosphorylation of
571 components of LHCII, but also of the PsbH subunit of PSII. Phosphorylation of LHCII still
572 occured in a mutant lacking PSII (Wollman and Delepelaire, 1984), but phosphorylation of
573 PSII did not occur in a mutant lacking LHCII proteins (Devitry and Wollman, 1988). While the
574 two phosphatases target partially overlapping sets of components of both PSII and LHCII, it
575 seems likely that differences in regulation and target specificities also lie with the protein
576 kinases STT7 and STL1. STT7 appears specific for LHCII (Turkina et al., 2006; Lemeille et
577 al., 2010), while putatively STL1 might phosphorylate PSII, like its paralog STN8 in
578 Arabidopsis (reviewed by (Rochaix et al., 2012)). We also obtained evidence that both
579 phosphatases are involved in the de-phosphorylation of PETO, which is implicated in the
580 control of cyclic electron flow (Takahashi et al., 2016). In summary, CrPBCP and CrPPH1
581 seem to have distinct but overlapping sets of targets, with CrPBCP having a somewhat wider
582 spectrum. Whether these targets represent direct substrates of the phosphatases, or indirect
583 targets through regulatory cascades cannot be determined from our genetic analysis.

584 In Chlamydomonas, LHCBM5, CP29 and CP26 were found to be enriched in PSI-LHCI-
585 LHCII complexes in St 2 (Takahashi et al., 2006; Takahashi et al., 2014), although all types

586 of LHCBM could also be found (Drop et al., 2014). Genetic studies have shown that type III
587 isoform LHCBM2/7, type I isoforms LHCBM4/6/8, as well as CP29 and CP26 are implicated
588 in state transitions (Tokutsu et al., 2009; Ferrante et al., 2012; Girolomoni et al., 2017;
589 Cazzaniga et al., 2020). We observed that, with the possible exception of LHCBM2/7, all
590 types of LHCBMs as well as LHCB4 and LHCB5 are differentially phosphorylated in St 2
591 compared to St 1. In particular we found that LHCBM1 was phosphorylated in St 2, that its
592 phosphorylation depends on STT7, and that it was de-phosphorylated in St 1, mainly reliant
593 on CrPPH1. However mutants which lack LHCBM1 were previously found to be able to
594 perform state transitions (Ferrante et al., 2012). Taken together these observations beg the
595 question of the physiological role of LHCBM1 phosphorylation. A possible explanation might
596 be that for state transitions LHCBM1 phosphorylation acts redundantly with the
597 phosphorylation of other antenna proteins, so that they can fulfill this role in the mutants
598 lacking LHCBM1. Analysis of knock-down mutants indicated that LHCBM2/7 is important for
599 state transitions (Ferrante et al., 2012). The comparison of the data we obtained with the
600 antibodies against LHCBM2/7 and LHCBM4/6/8, suggests that the type III isoform
601 LHCBM2/7 may not be phosphorylated in St 2, consistently with the previous report that
602 phosphorylation of LHCBM2/7 is not detected in the PSI-LHCI-LHCII complex (Drop et al.,
603 2014). A possible reason might be that LHCBM2/7 could be required structurally for the
604 association of LHCII trimers to PSI-LHCI, but that this isoform would not be involved in
605 regulation through phosphorylation. This would be analogous to the case in Arabidopsis,
606 where Lhcb1 is not phosphorylated when part of the mobile LHCII trimer that binds PSI-
607 LHCI, so that it is only the phosphorylation of Lhcb2 that is required for binding to the PSI
608 docking site (Crepin and Caffarri, 2015; Longoni et al., 2015; Pan et al., 2018).

609 Compared to Arabidopsis, Chlamydomonas lacks LHCB6 (CP24), but has a more complex
610 complement of the LHCBM subunits composing the LHCII trimers (reviewed by (Crepin and
611 Caffarri, 2018)). Another difference is that in Chlamydomonas, some PSI-LHCI-LHCII
612 complexes contain not only LHCII trimers but also the “minor” antennae LHCB4 and LHCB5
613 (Drop et al., 2014; Takahashi et al., 2014). Furthermore the amplitude of state transitions is
614 larger in Chlamydomonas than in plants (Delosme et al., 1996), and in the alga strong state
615 transitions are induced by changes in metabolic demands for ATP or reducing power, for
616 example under anoxic conditions (Bulte and Wollman, 1990; Cardol et al., 2009). It remains
617 a matter of speculation whether these differences are related to the more intricate roles of
618 the phosphatases CrPPH1 and CrPBCP in the regulation of light harvesting that have
619 evolved in Chlamydomonas. On the other hand, in Chlamydomonas, phosphorylation of
620 LHCB4 is controlled by CrPBCP, reminiscent of monocots such as rice where
621 phosphorylation of LHCB4 is controlled by OsSTN8 and OsPBCP (Betterle et al., 2017).

Further “evo-physio” investigations from a combined evolutionary and physiological perspective on the role of protein phosphorylation in the regulation of photosynthetic acclimation in diverse organisms promise to be a fertile approach.

MATERIAL AND METHODS

Strains, growth conditions, and media

The *cw15.16 (mt +)* mutant was obtained by crossing *cw15 (mt -)* to wild type 137C. The *C. reinhardtii* CLiP strain LMJ.RY0402.16176, its parental strain CC4533 (mt -) and the corresponding strain of opposite mating type CC5155 (*mt* +) were obtained from the Chlamydomonas Resource Center (https://www.chlamycollection.org/) (Li et al., 2016). This CLiP strain (*pph1;cao*) was backcrossed twice to CC4533, and then to *cw15* to obtain the cell-wall deficient mutant strain *pph1;cw15* used in this work, and referred to as *pph1*. The *pbcp* strain was isolated by screening random insertional mutants for aberrant chlorophyll-fluorescence induction kinetics. These mutants were generated by inserting an *aphVIII* cassette in wild type 137C (mt-) (Tolleter et al., 2011). The *pbcp* mutant was backcrossed with wild type 137C (mt+), and further to *cw15.16 (mt+)* to obtain the cell-wall deficient mutant strain *pbcp;cw15* used in this work, and referred to as *pbcp*. The genotype of the progeny was verified by PCR (see below) and the phenotype by monitoring state transitions using PAM chlorophyll fluorescence spectroscopy (see below).

Cells were grown in Tris acetate phosphate (TAP) (Harris et al., 1989) under normal growth light (60 - 80 µmol m^{-2} s^{-1}) from white fluorescent tubes. The state transitions were obtained with cells in exponential growth phase (2-3 10^6 cells/mL) collected by centrifugation, resuspended in High Salt Minimal medium (HSM) at a concentration of 2-3 10^7 cells/mL, and pre-acclimated in dim light (~10 µmol m^{-2} s^{-1}) for 2 h with shaking.

Mapping of the insertion in *pbcp*

DNA was isolated using the CTAB method and quantified using a NanoDrop spectrophotometer (ThermoScientific). The Resda-PCR protocol was used to identify the left border, the technique was adapted from (Gonzalez-Ballester et al., 2005). The first PCR is performed with Taq polymerase and 10% DMSO. The primers and the program used are described in Table X and Y. A nested PCR was performed on the product of the first PCR diluted to 1/1000, 1/500 or 1/50 using KOD polymerase Xtreme™ (MerckMillipore). The product of the second PCR was then loaded onto an agarose gel 2% and fragments with a molecular weight greater than 800 bp were isolated. PCR products were extracted from the gel and purified with NucleoSpin® Gel and PCR Clean-up Kit (Macherey Nagel) and eluted

656 in water. The Genome Walker technique (Clonetech) was used to identify the right border of
657 the flanking sequence of the cassette insertion site. Genomic DNA was successively
658 digested using the enzyme PvuII followed by the ligation of a specific adapter. The primary
659 PCR uses a primer specific to the insert (AphVIII) and an adapter specific primer. This was
660 followed by a nested PCR whereby products greater than 800 bp are extracted from agarose
661 gel and cloned. Cloning of The PCR products were performed in the vector pGEM®-T
662 (Promega) containing the lactose operon and the gene coding for ampicillin resistance and
663 then transformed into chemocompetent bacteria (DH5) by thermal shock. The bacteria were
664 selected on LB Ampicillin medium in the presence of IPTG (ß-D-1-ThioGalactopyranoside
665 and X-Gal (5-bromo-4-chloro-3-indolyl-beta-D-galactopyranoside) to allow for white/blue
666 selection.

667 **DNA Constructs**

668 The closest homolog of Arabidopsis thaliana PPH1/TAP38 (At4G27800) was identified in *C.*
669 *reinhardtii* as Cre04.g218150 in reciprocal BLAST searches performed in Phytozome 12 (E-
670 value: 6. E-57; https://phytozome.jgi.doe.gov/pz/portal.html#!search?show=BLAST) and
671 TAIR 10 (E-value: 9. E-56; http://www.arabidopsis.org/Blast/index.jsp).

672 Vector pPL18 was obtained from pSL18 by replacing the *aphVIII* resistance cassette with the
673 hygromycin resistance cassette. (Sizova et al., 2001). For this the *aphVIII* cassette was
674 removed by KpnI / XhoI digestion. The hygromycin cassette was amplified from plasmid
675 MAC1_gen3 (Douchi et al., 2016) with primers pPL_56 and pPL_57 (see Table S2) and
676 cloned by Gibson assembly (Gibson et al. (2009)).

677 The vector was further modified to allow the fusion of a triple HA (hemagglutinin) epitope tag
678 at the C-terminus of the coding sequences of interest. A synthetic fragment encoding the
679 triple epitope (obtained from Biomatik) was cloned into pPL18 by BsmI / NotI digestion,
680 yielding vector pFC18.

681 The *CrPPH1* coding sequence (CDS) was amplified from a Chlamydomonas cDNA library
682 with primers pFC_216 and pFC_217 and cloned by Gibson assembly into pFC18 linearized
683 with EcoRV / BglII, resulting in pFC18_CrPPH1_HA. The *CrPBCP* CDS was amplified from a
684 cDNA library with primers pFC_218 and pFC_219 and cloned as above into pFC18 resulting
685 in pFC18_CrPBCP_HA. The *CrPPH1* CDS without the predicted chloroplast transit peptide
686 (cTP) was amplified with primer pFC_265 and primer pFC_266 from pFC18_CrPPH1_HA,
687 then cloned into vector pet28a digested with NdeI and SalI to obtain pet28a_CrPPH1_ΔcTP.
688 The *CrPBCP* CDS without the predicted cTP was amplified with primer pFC_267 and primer
689 pFC_268 from pFC18_CrPBCP_HA, and cloned into pet28a as above to obtain
690 pET28a_CrPBCP_ΔcTP. All vectors used were verified by sequencing.

691 **Transformation**

692 Nuclear transformation by electroporation was modified from (Shimogawara et al., 1998).
693 Cells in exponential phase were collected by centrifugation and resuspended at 10^8 cell/mL
694 in TAP + 60 mM Sucrose. A volume of 300 µL of cells was incubated with 1 µg plasmid DNA
695 (linearized with XbaI) at 16°C for 20 min, and then the mix was transferred to a 4-mm-gap
696 electroporation cuvette and pulsed at 500 V (C = 50 µF) using a BioRad electroporator
697 (GenePulser II). The cuvette was then incubated at 16°C for 20 min. The cell suspension
698 was diluted into 20 mL TAP, incubated in dim light with gentle agitation for 16h, and
699 collected by centrifugation prior to plating and selection on TAP + 25 µg mL^{-1} hygromycin
700 (Sigma).

701 **Production of polyclonal antiserum of CrPPH1, CrPBCP, and LHCBMs**

702 For production of CrPPH1 and CrPBCP, recombinant proteins were expressed from
703 plasmids pet28a-CrPPH1_ΔcTP and pET28a-CrPBCP_ΔcTP in *Escherichia coli* BL21(DE3),
704 induced with 1mM IPTG for 4 hours at 37°C. Recombinant proteins purified as in (Ramundo
705 et al., 2013) were used to immunize rabbits and antisera were purified by affinity
706 chromatography with the corresponding protein (Eurogentec).

707 For production of anti-peptide antisera targeting different LHCBMs isoforms (Natali and
708 Croce, 2015), synthetic peptides (Fig. S9) were used for rabbit immunization and affinity
709 chromatography (Eurogentec). For assessing the specificity and cross-reaction of the
710 antibodies, pET28a plasmids carrying the coding sequences of LHCBM1, LHCBM2,
711 LHCBM3, LHCBM4, LHCBM5, LHCBM6, LHCBM9, CP26 and CP29 (Girolomoni et al.,
712 2017) were used to express all the antenna proteins in *E. coli* BL21(DE3).

713 **Fluorescence Measurements**

714 Maximum quantum efficiency of PSII (Fv/Fm) of cells that were adapted for ~1 to 5 min in
715 the dark was measured with a plant efficiency analyzer (Handy PEA; Hansatech
716 Instruments) with the parameters recommended by the manufacturer. State transitions were
717 monitored with a pulse amplitude modulation fluorometer (PAM-Hansatech). A 2 ml sample
718 of cells grown and pre-acclimated in HSM as described above was transferred to the dark in
719 the vessel of a pulse amplitude modulation fluorometer (PAM, Hansatech). The sample was
720 kept in the dark with stirring, and saturating pulses (pulse width of 0.7 sec; intensity 85 %)
721 were applied every 4 minutes. The St 1 to St 2 transition was induced by sealing the
722 chamber, so that respiration led to anoxic conditions, and then the transition from St 2 to St 1
723 was induced by bubbling air in the sample. The alternate protocol for inducing state
724 transitions in the presence of DCMU is described in Fig. S4. Chlorophyll fluorescence

725 emission spectra at 77 K were measured with a spectrofluorometer (Ocean Optics) with
726 excitation from a LED light source at 435 nm.

727 **Immunoblotting**

728 For total protein extraction, cells in exponential phase were collected by centrifugation,
729 resuspended in lysis buffer (50 mM Tris-HCl, pH 6.8, 2% SDS, and 10 mM EDTA) and 1×
730 Protease inhibitor cocktail (Sigma-Aldrich) and incubated at 37°C for 30 min with shaking in
731 a thermomixer. Cell debris were removed by centrifugation at 16 000*g* for 10 min at 4°C and
732 the supernatant was used as total protein extract. For protein phosphorylation analysis, any
733 centrifugation step of living cells was avoided by instantly dousing the cultures in 4 volumes
734 of cold acetone. After 30 min incubation on ice and centrifugation at 12 000*g* for 12 min in a
735 SLA-4 rotor (Sorvall), the pellet was treated as before. Samples (10 or 50 µg of total protein)
736 were denaturated for 30 min at 37°C prior to SDS-PAGE (Laemmli, 1970) in 15 or 12%
737 acrylamide gels. After wet transfer the nitrocellulose membranes (Biorad) were blocked in
738 Tris-buffered saline plus Tween (TBST; 20 mM Tris, pH 7.5, 150 mM NaCl, and 0.1% [v/v]
739 Tween 20) supplemented with 5% (w/v) nonfat milk (or 3% (w/v) BSA in case of anti-
740 Phospho-Thr immunoblotting), for 2h at room temperature or 16h at 4°C.

741 The antisera (and their sources) were as follows: monoclonal anti-HA (Promega), anti-
742 phospho-LHCB2 (Agrisera; AS13-2705), anti-PsaA (a gift of Kevin Redding), anti-Cytf, anti-
743 D1 (gifts of Jean-David Rochaix), anti-Phospho Thr (Invitrogen), anti-LHCB4, anti-LHCB5,
744 anti-LHCBM5 (gifts of Yuichiro Takahashi), anti-rabbit IgG horseradish peroxidase conjugate
745 (Promega), anti-mouse IgG horseradish peroxidase conjugate (Promega). For primary
746 antibody decoration, antibodies were diluted in the same buffers as for blocking and
747 incubation was for 2 hours at room temperature or 16 hours at 4°C. Membranes were
748 washed 4 times for 8 minutes with TBS-T and then incubated 1 hour at room temperature
749 with horseradish-peroxidase conjugated secondary antibody diluted in TBS-T with 5% (w/v)
750 nonfat milk (or 3% (w/v) BSA in case of anti-Phospho Thr immunoblotting). Membranes were
751 washed 4 times for 8 minutes with TBS-T and then revealed by enhanced
752 chemiluminescence (ECL).

753 **Phos-Tag Gel Electrophoresis**

754 Double layer Phos-tag gels (12 % acrylamide / bisacrylamide 37.5:1; 65 uM Phos Tag) were
755 prepared as in (Longoni et al., 2015) except that the presence of EDTA in the lysis buffer
756 was compensated by adding equimolar $Zn(NO_3)_2$ to the samples, and denaturated for 30 min
757 at 37°C before loading. Protein dephosphorylation on the membranes was performed as in
758 (Longoni et al., 2015). For *in vitro* dephosphorylation, a cell pellet was resuspended in 5mM
759 Hepes pH 7.5, 10 mM EDTA, 1 % TritonX 100; and an aliquot containing 10 µg protein was

760 treated with lambda protein phosphatase reaction mix following the instructions of the
761 manufacturer (New England Biolabs) for 1 h at 30°C.

762

763 **ACKNOWLEDGMENTS**

764 This research was funded by the Marie Curie Initial Training Network project, AccliPhot
765 (grant agreement number PITN-GA-2012-316427), the University of Geneva, the Institute of
766 Genetics and Genomics of Geneva (iGE3), the Swiss National Science Foundation (SNF
767 31003A_146300), the European FP6 program (SOLAR-H Project STRP516510) and the
768 Agence Nationale pour la Recherche (ChloroPaths : ANR-14-CE05-0041-01). M.C. was
769 supported by a scholarship from the Ministry of Science and Education.

770 We thank Jean-David Rochaix, Jean Alric, Bernard Genty and Gilles Peltier for scientific
771 advice, Pascaline Auroy for technical assistance, Matteo Ballottari for the plasmids
772 expressing LHCBMs, Francis-André Wollman for antiserum against PETO, Yuichiro
773 Takahashi for antisera against CP29, CP26 and LHCBM5, and Nicolas Roggli for help with
774 preparing the figures.

775 The authors declare no conflict of interest.

776

777

FIGURE LEGENDS

Fig. 1. Characterization of the *pph1* mutant

A) Schematic representation of the *PPH1* gene. Exons are represented as black boxes, introns as black lines and the 5'UTR and 3'UTR as white boxes. The arrowhead indicates the site of insertion of the CIB1 cassette in intron 7.

B) Immunoblot analysis. Total protein extracts (50 µg) of the wild type (WT) and of the *pph1* mutant were subjected to SDS-PAGE and immunoblotting with antisera against CrPPH1 or AtpB (loading control).

C) 77 K chlorophyll fluorescence emission spectra under conditions that favor St 2 (anaerobiosis in the dark) and after 20 min under conditions that favor St 1 (strong aeration). The data are normalized on the PSII peak at 680 nm.

D) State transitions monitored by PAM chlorophyll fluorescence spectroscopy at room temperature. Saturating light flashes were fired every four minutes and fluorescence was measured continuously (no actinic light was applied). Data were normalized on the first Fm' peak. The transition from St 1 to St 2 was induced by sealing the sample chamber to allow respiration to deplete oxygen and cause anoxic conditions, and then the transition from St 2 to St 1 was induced by bubbling air in the sample (at the time indicated with a black arrow).

E) Phospho-immunoblot analysis. Total protein extracts (10 µg) of wild type and *pph1* cells in conditions favoring St 2 or St 1 (as in panel B) were subjected to SDS-PAGE and immunoblotting with antisera against P-Thr, P-Lhcb2 or AtpB (loading control).

Fig. 2. Complementation of the *pph1* mutant

A) Immunoblot analysis. Total protein extracts (50 µg) of the wild type, the *pph1* mutant and four complemented lines (*pph1:PPH1-HA*) were subjected to SDS-PAGE and immunoblotting with antisera against CrPPH1, the HA epitope and D1 (loading control).

B) State transitions in the *pph1* mutant and two complemented lines were monitored by PAM chlorophyll fluorescence spectroscopy as in Figure 1D.

C) Phospho-immunoblot analysis. Total protein extracts (10 µg) of the *pph1* mutant and of complemented lines were subjected to SDS-PAGE and immunoblotting with antisera against P-Thr or AtpB (loading control).

Fig. 3 Characterization of the *pbcp* mutant

A) Schematic representation of the *PBCP* gene. Exons are represented as black boxes, introns as black lines and 3'UTR / 5'UTR as white boxes. The arrow indicates the site of insertion of the *aphVIII* cassette in exon 2.

B) Immunoblot analysis. Total protein extracts of the wild type and of the *pbcp* mutant (50 µg) were subjected to SDS-PAGE and immunoblotting with antisera against PBCP or AtpB (loading control).

C) 77 K chlorophyll fluorescence emission spectra under condition that favor St 2 and after 20 min under conditions that favor St 1, as in Fig 1C.

818 D) State transitions of the wild type (WT) and the *pbcp* mutant were monitored by PAM
819 chlorophyll fluorescence spectroscopy as in Figure 1D.

820 E) Phospho-immunoblot analysis of state transitions. Total protein extracts of wild type and
821 *pbcp* cells in St 2 and St 1 (10 µg, treated as in panel 2 C)) were subjected to SDS-PAGE
822 and immunoblotting with antisera against P-Thr, P-Lhcb2 or AtpB (loading control).

823 F) Phospho-immunoblot analysis of light acclimation. The cells were grown in low light and
824 then transferred to the dark (D), growth light (GL, 80 µE m^{-2} s^{-1}) or high light (HL, 300 µE m^{-2}
825 s^{-1}) for 2 hours and analyzed like in panel E).

826

827 **Fig. 4. Complementation of the *pbcp* mutant**

828 A) Immunoblot analysis. Total protein extracts (50 µg) of the wild type, the *pbcp* mutant and
829 four complemented lines (*pbcp:PBCP-HA*) were subjected to SDS-PAGE and
830 immunoblotting with antisera against CrPBCP, the HA epitope or AtpB (loading control).

831 B) State transitions in the *pbcp* mutant and two complemented lines were monitored by PAM
832 chlorophyll fluorescence spectroscopy at room temperature as in Figure 1D.

833 C) Phospho-immunoblot analysis. Total protein extracts (10 µg) of the *pbcp* mutant and of
834 complemented lines were subjected to SDS-PAGE and immunoblotting with antisera against
835 P-Lhcb2, P-Thr and AtpB (loading control).

836

837 **Fig. 5. Characterization of the *pph1;pbcp* double mutant**

838 A) Immunoblot analysis. Total protein extracts(50 µg) of the wild type, *stt7*, *pph1* and *pbcp*,
839 *pph1;pbcp* (clones # 46A and #50C) were subjected to SDS-PAGE and immunoblotting with
840 antisera against STT7, AtpB (loading control), CrPPH1 and CrPBCP.

841 B) State transitions of the wild type (WT) and two *pph1;pbcp* mutants were monitored by
842 PAM chlorophyll fluorescence spectroscopy at room temperature, as in Figure 1D. The data
843 were not normalized to the first Fm' peak.

844 C) Phospho-immunoblot analysis. Total protein extracts of wild type and *pph1;pbcp* cells in
845 conditions favoring St 1, then St 2 and finally again St1 (10 µg; cells treated as in panel 1C)
846 were subjected to SDS-PAGE and immunoblotting with antisera against P-Thr, P-Lhcb2 or
847 AtpB (loading control).

848 D) 77 K chlorophyll fluorescence emission spectra under conditions sequentially favoring St
849 1, St 2 and St1, obtained as in Fig 1C.

850

851 **Fig. 6. Analysis of CrPPH1 and CrPBCP targets**

852 A) Phospho-immunoblot analysis. Total protein extracts of *stt7*, wild type, *pph1*, *pbcp*,
853 *pph1;pbcp* (10 µg) in conditions favoring St 2 and then St 1 were subjected to SDS-PAGE
854 and immunoblotting with antisera against P-Thr or AtpB (loading control).

855 B) Phos-tag PAGE and immunoblot analysis. Total protein extracts (10 µg) of *stt7*, wild type,
856 *pph1*, *pbcp*, or *pph1;pbcp* in St 2 and then St 1 were subjected to Phos-tag PAGE and
857 immunoblotting with antisera against LHCBM1, LHCBM3, LHCBM4/6/8, LHCBM2/7,
858 LHCBM5, LHCB4, LHCB5, PsbH or PETO. A sample of the wild type in state 2 was treated

859 with lambda phosphatase (+λ) and used as a reference for the migration of the non-
860 phosphorylated form (NP). The migration of the phosphorylated forms (P) is retarded by the
861 Phos-tag immobilized in the polyacrylamide gel.

862

863

864 Supplemental Data

865 **Fig. S1. Genotyping of two insertions in the *pph1* mutant and segregation analysis**

866 **Fig. S2. Growth properties of the single and double mutants**

867 **Fig. S3. Validation of CrPPH1 and CrPBCP antisera**

868 **Fig. S4. Time course of state transitions in the presence of DCMU and corresponding**
869 **fluorescence emission spectra at 77 K**

870 **Fig. S5. Migration of selected thylakoid proteins following SDS-PAGE**

871 **Fig. S6. Identification of the *pbcp* mutant and segregation analysis**

872 **Fig. S7. Genotyping of *pph1;pbcp* double mutants**

873 **Fig. S8. Accumulation of photosynthetic proteins in the single and double mutants**

874 **Fig. S9. Design of peptide antigens for antisera against LHCBM isoforms**

875 **Fig. S10. Specificity and cross-reactions of the antisera against LHCII components**

876 **Table S1. Chlorophyll content and maximum quantum yield of PSII in the phosphatase**
877 **mutants**

878 **Table S2. List of oligonucleotides used in this work**

879

880
881

882

Figure 1

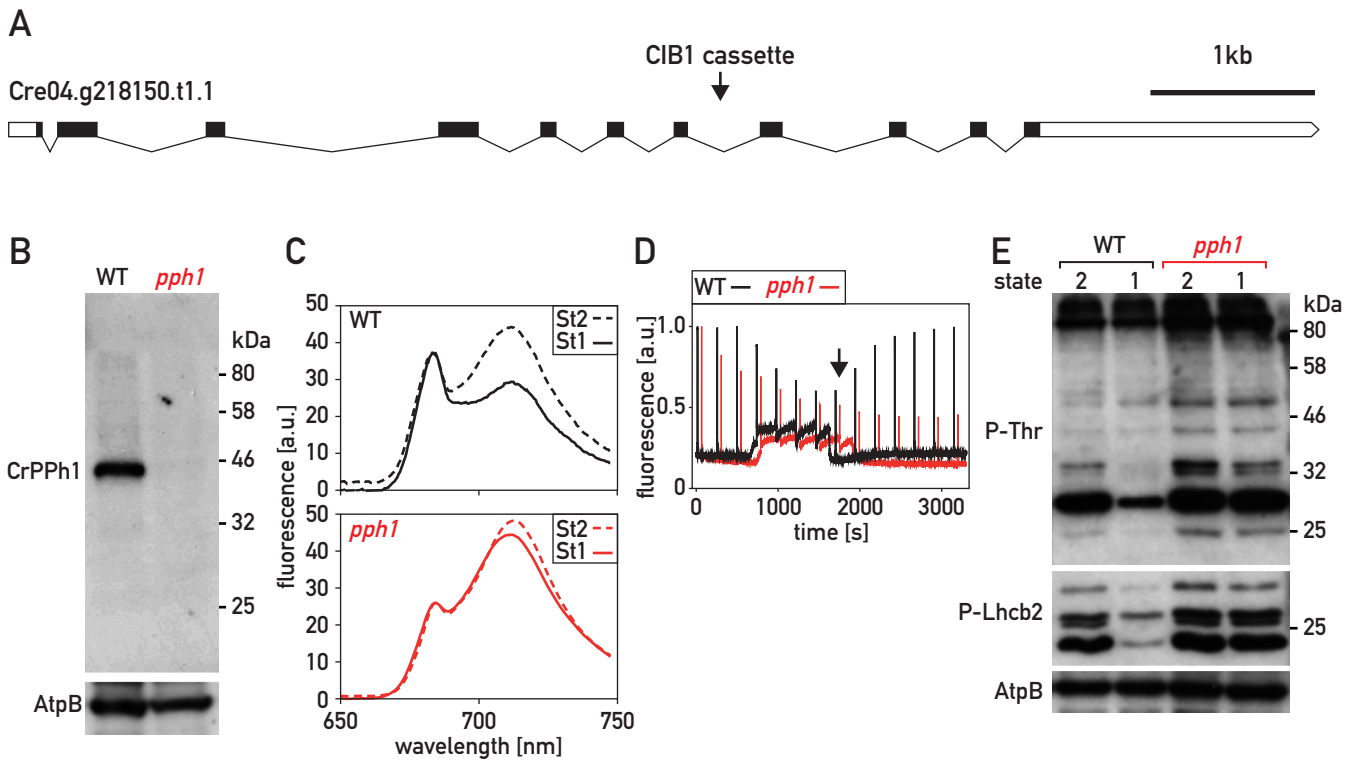

Fig. 1. Characterization of the *pph1* mutant

A) Schematic representation of the *PPH1* gene. Exons are represented as black boxes, introns as black lines and the 5'UTR and 3'UTR as white boxes. The arrowhead indicates the site of insertion of the CIB1 cassette in intron 7.

B) Immunoblot analysis. Total protein extracts (50 µg) of the wild type (wt) and of the *pph1* mutant were subjected to SDS-PAGE and immunoblotting with antisera against CrPPH1 or AtpB (loading control).

C) 77 K chlorophyll fluorescence emission spectra under conditions that favor St 2 (anaerobiosis in the dark) and after 20 min under conditions that favor St 1 (strong aeration). The data are normalized on the PSII peak at 680 nm.

D) State transitions monitored by PAM chlorophyll fluorescence spectroscopy at room temperature. Saturating light flashes were fired every four minutes and fluorescence was measured continuously (no actinic light was applied). Data were normalized on the first Fm' peak. The transition from St 1 to St 2 was induced by sealing the sample chamber to allow respiration to deplete oxygen and cause anoxic conditions, and then the transition from St 2 to St 1 was induced by bubbling air in the sample (at the time indicated with a black arrow).

E) Phospho-immunoblot analysis. Total protein extracts (10 µg) of wild type and *pph1* cells in conditions favoring St 2 or St 1 (as in panel B) were subjected to SDS-PAGE and immunoblotting with antisera against P-Thr, P-Lhcb2 or AtpB (loading control).

Figure 2

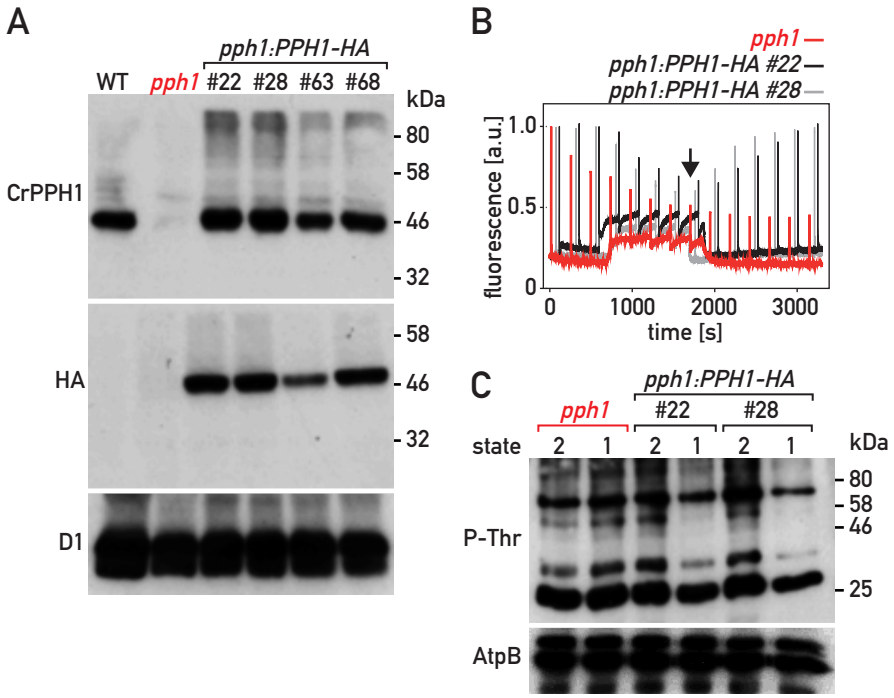

Fig. 2. Complementation of the *pph1* mutant

A) Immunoblot analysis. Total protein extracts (50 µg) of the wild type, the *pph1* mutant and four complemented lines (*pph1:PPH1-HA*) were subjected to SDS-PAGE and immunoblotting with antisera against CrPPH1, the HA epitope and D1 (loading control).

B) State transitions in the *pph1* mutant and two complemented lines were monitored by PAM chlorophyll fluorescence spectroscopy as in Figure 1D.

C) Phospho-immunoblot analysis. Total protein extracts (10 µg) of the *pph1* mutant and of complemented lines were subjected to SDS-PAGE and immunoblotting with antisera against P-Thr or AtpB (loading control).

Figure 3

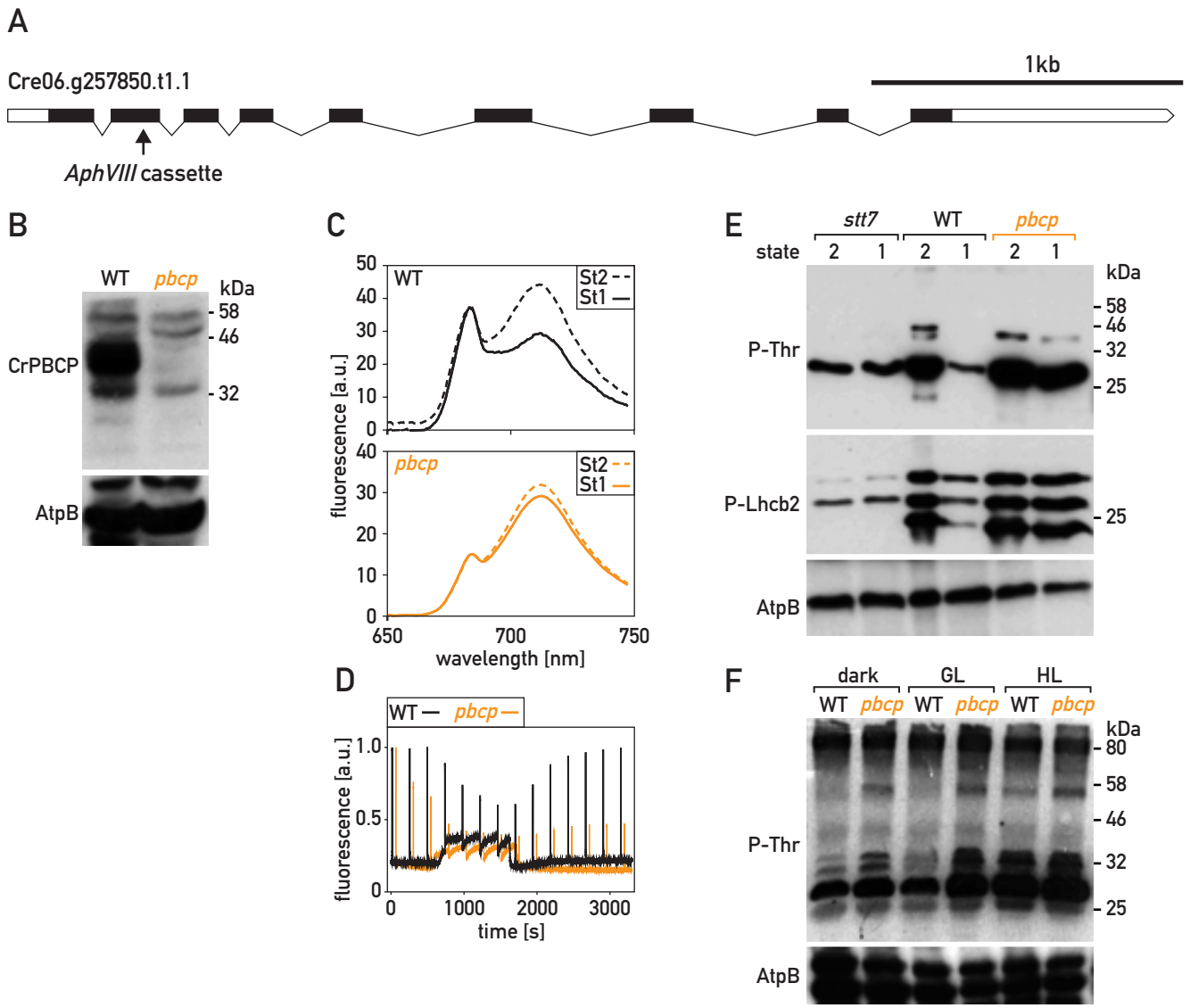

Fig. 3 Characterization of the *pbcp* mutant

A) Schematic representation of the *PBCP* gene. Exons are represented as black boxes, introns as black lines and 3'UTR / 5'UTR as white boxes. The arrow indicates the site of insertion of the *aphVIII* cassette in exon 2.

B) Immunoblot analysis. Total protein extracts of the wild type and of the *pbcp* mutant (50 µg) were subjected to SDS-PAGE and immunoblotting with antisera against PBCP or AtpB (loading control).

C) 77 K chlorophyll fluorescence emission spectra under condition that favor St 2 and after 20 min under conditions that favor St 1, as in Fig 1C.

D) State transitions of the wild type (WT) and the *pbcp* mutant were monitored by PAM chlorophyll fluorescence spectroscopy as in Figure 1D.

E) Phospho-immunoblot analysis of state transitions. Total protein extracts of wild type and *pbcp* cells in St 2 and St1 (10 µg, treated as in panel 2 C)) were subjected to SDS-PAGE and immunoblotting with antisera against P-Thr, P-Lhcb2 or AtpB (loading control).

F) Phospho-immunoblot analysis of light acclimation. The cells were grown in low light and then transferred to the dark (D), growth light (GL, 80 µE m^{-2} s^{-1}) or high light (HL, 300 µE m^{-2} s^{-1}) for 2 hours and analyzed like in panel E).

Figure 4

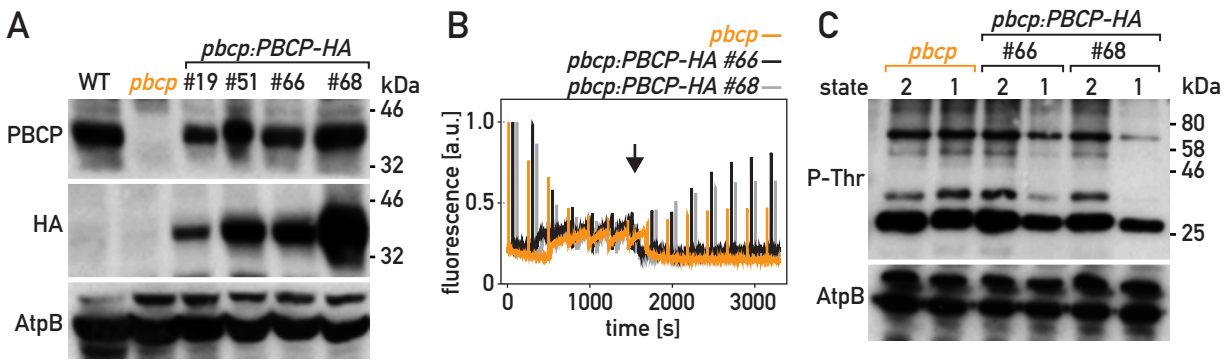

Fig. 4. Complementation of the *pbcp* mutant

A) Immunoblot analysis. Total protein extracts (50 µg) of the wild type, the *pbcp* mutant and four complemented lines (*pbcp:PBCP-HA*) were subjected to SDS-PAGE and immunoblotting with antisera against CrPBCP, the HA epitope or AtpB (loading control).

B) State transitions in the *pbcp* mutant and two complemented lines were monitored by PAM chlorophyll fluorescence spectroscopy at room temperature as in Figure 1D.

C) Phospho-immunoblot analysis. Total protein extracts (10 µg) of the *pbcp* mutant and of complemented lines were subjected to SDS-PAGE and immunoblotting with antisera against P-Lhcb2, P-Thr and AtpB (loading control).

Figure 5

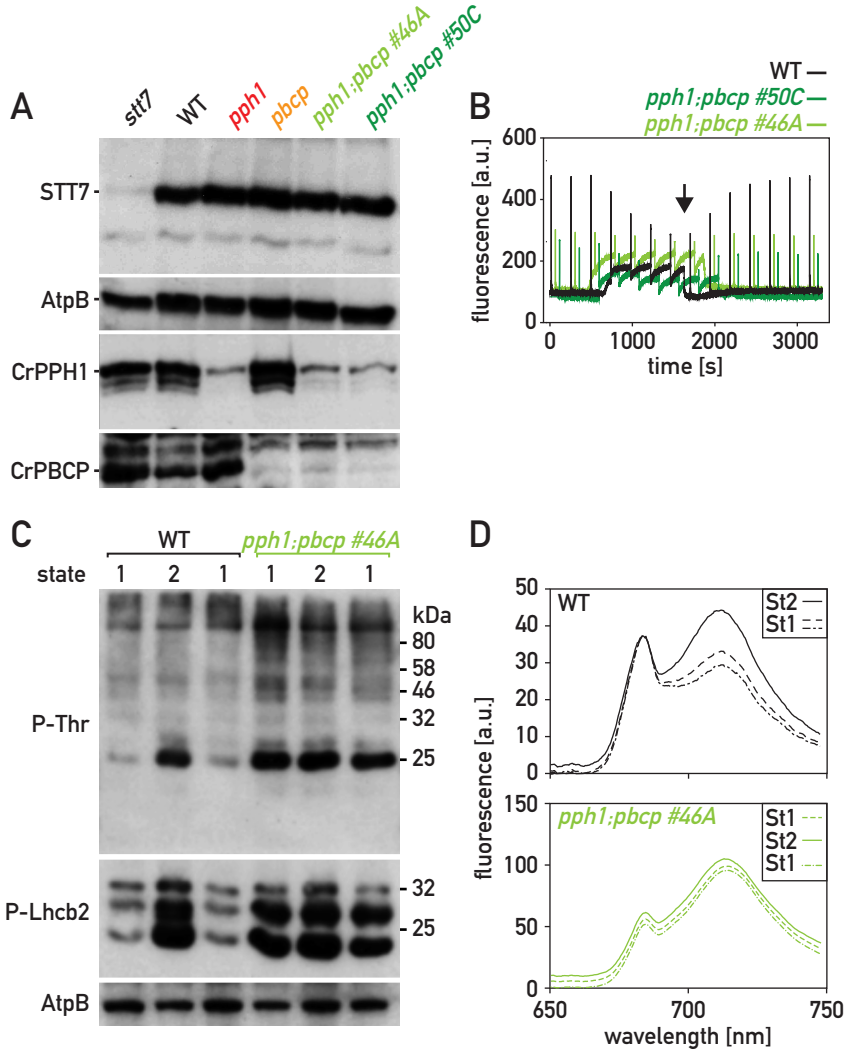

Fig. 5. Characterization of the *pph1;pbcp* double mutant

A) Immunoblot analysis. Total protein extracts(50 µg) of the wild type, *stt7*, *pph1* and *pbcp*, *pph1;pbcp* (clones # 46A and #50C) were subjected to SDS-PAGE and immunoblotting with antisera against STT7, AtpB (loading control), CrPPH1 and CrPBCP.

B) State transitions of the wild type (WT) and two *pph1;pbcp* mutants were monitored by PAM chlorophyll fluorescence spectroscopy at room temperature, as in Figure 1D. The data were not normalized to the first Fm' peak.

C) Phospho-immunoblot analysis. Total protein extracts of wild type and *pph1;pbcp* cells in conditions favoring St 1, then St 2 and finally again St 1 (10 µg; cells treated as in panel 1C) were subjected to SDS-PAGE and immunoblotting with antisera against P-Thr, P-Lhcb2 or AtpB (loading control).

D) 77 K chlorophyll fluorescence emission spectra under conditions sequentially favoring St 1, St 2 and St 1, obtained as in Fig 1C.

Figure 6

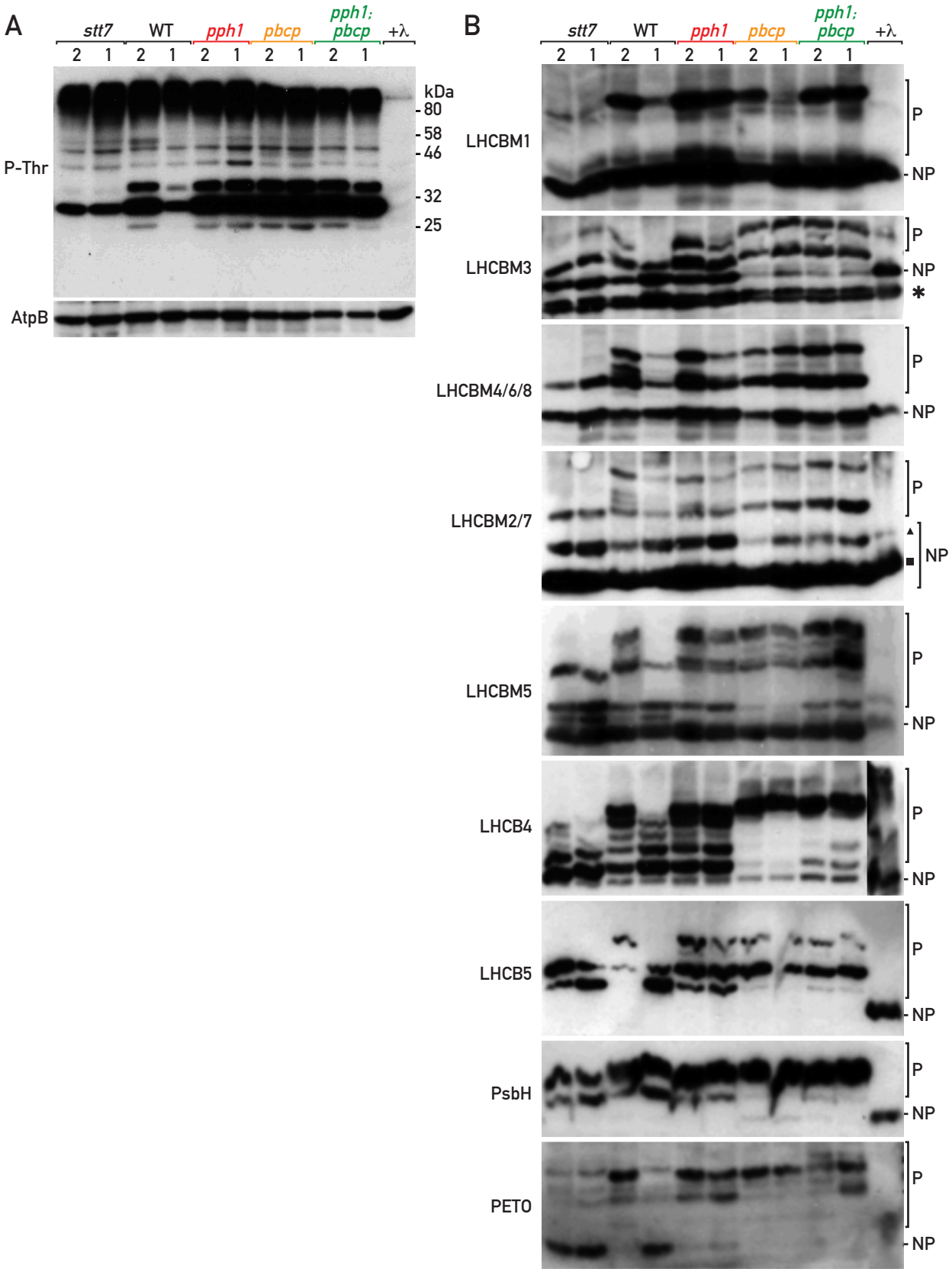

Fig. 6. Analysis of CrPPH1 and CrPBCP targets

A) Phospho-immunoblot analysis. Total protein extracts of *stt7*, wild type, *pph1*, *pbcp*, *pph1;pbcp* (10 µg) in conditions favoring St 2 and then St 1 were subjected to SDS-PAGE and immunoblotting with antisera against P-Thr or AtpB (loading control).

B) Phos-tag PAGE and immunoblot analysis. Total protein extracts (10 µg) of *stt7*, wild type, *pph1*, *pbcp*, or *pph1;pbcp* in St 2 and then St 1 were subjected to Phos-tag PAGE and immunoblotting with antisera against LHCBM1, LHCBM3, LHCBM4/6/8, LHCBM2/7, LHCBM5, LHCB4, LHCB5, PsbH or PETO. A sample of the wild type in state 2 was treated with lambda phosphatase (+λ) and used as a reference for the migration of the non-phosphorylated form (NP). The migration of the phosphorylated forms (P) is retarded by the Phos-tag immobilized in the polyacrylamide gel. Bands marked with an asterisk, a triangle and a square are discussed in the main text.

Parsed Citations

Bassi R, Wollman FA (1991) The chlorophyll-a/b proteins of photosystem II in Chlamydomonas reinhardtii : Isolation, characterization and immunological cross-reactivity to higher-plant polypeptides. Planta 183: 423-433
Pubmed: Author and Title
Google Scholar: Author Only Title Only Author and Title

Bellafiore S, Barneche F, Peltier G, Rochaix JD (2005) State transitions and light adaptation require chloroplast thylakoid protein kinase STN7. Nature 433: 892-895
Pubmed: Author and Title
Google Scholar: Author Only Title Only Author and Title

Benson SL, Maheswaran P, Ware MA, Hunter CN, Horton P, Jansson S, Ruban AV, Johnson MP (2015) An intact light harvesting complex I antenna system is required for complete state transitions in Arabidopsis. Nat Plants 1: 15176
Pubmed: Author and Title
Google Scholar: Author Only Title Only Author and Title

Betterle N, Ballottari M, Baginsky S, Bassi R (2015) High light-dependent phosphorylation of photosystem II inner antenna CP29 in monocots is STN7 independent and enhances nonphotochemical quenching. Plant Physiol 167: 457-471
Pubmed: Author and Title
Google Scholar: Author Only Title Only Author and Title

Betterle N, Poudyal RS, Rosa A, Wu G, Bassi R, Lee CH (2017) The STN8 kinase-PBCP phosphatase system is responsible for high-light-induced reversible phosphorylation of the PSII inner antenna subunit CP29 in rice. Plant J 89: 681-691
Pubmed: Author and Title
Google Scholar: Author Only Title Only Author and Title

Buchert F, Hamon M, Gabelein P, Scholz M, Hippler M, Wollman FA (2018) The labile interactions of cyclic electron flow effector proteins. J Biol Chem 293: 17559-17573
Pubmed: Author and Title
Google Scholar: Author Only Title Only Author and Title

Bulte L, Gans P, Rebeille F, Wollman FA (1990) Atp Control on State Transitions Invivo in Chlamydomonas-Reinhardtii. Biochimica Et Biophysica Acta 1020: 72-80
Pubmed: Author and Title
Google Scholar: Author Only Title Only Author and Title

Bulte L, Wollman FA (1990) Stabilization of State-I and State-Ii by P-Benzoquinone Treatment of Intact-Cells of Chlamydomonas-Reinhardtii. Biochimica Et Biophysica Acta 1016: 253-258
Pubmed: Author and Title
Google Scholar: Author Only Title Only Author and Title

Cardol P, Alric J, Girard-Bascou J, Franck F, Wollman FA, Finazzi G (2009) Impaired respiration discloses the physiological significance of state transitions in Chlamydomonas. Proc Natl Acad Sci U S A 106: 15979-15984
Pubmed: Author and Title
Google Scholar: Author Only Title Only Author and Title

Cazzaniga S, Kim M, Bellamoli F, Jeong J, Lee S, Perozeni F, Pompa A, Jin E, Ballottari M (2020) Photosystem II antenna complexes CP26 and CP29 are essential for nonphotochemical quenching in Chlamydomonas reinhardtii. Plant Cell Environ 43: 496-509
Pubmed: Author and Title
Google Scholar: Author Only Title Only Author and Title

Crepin A, Caffarri S (2015) The specific localizations of phosphorylated Lhcb1 and Lhcb2 isoforms reveal the role of Lhcb2 in the formation of the PSI-LHCII supercomplex in Arabidopsis during state transitions. Biochim Biophys Acta 1847: 1539-1548
Pubmed: Author and Title
Google Scholar: Author Only Title Only Author and Title

Crepin A, Caffarri S (2018) Functions and Evolution of Lhcb Isoforms Composing LHCII, the Major Light Harvesting Complex of Photosystem II of Green Eukaryotic Organisms. Curr Protein Pept Sci 19: 699-713
Pubmed: Author and Title
Google Scholar: Author Only Title Only Author and Title

de Vitry C, Diner BA, Popo JL (1991) Photosystem II particles from Chlamydomonas reinhardtii. Purification, molecular weight, small subunit composition, and protein phosphorylation. J Biol Chem 266: 16614-16621
Pubmed: Author and Title
Google Scholar: Author Only Title Only Author and Title

Delepelaire P (1984) Partial characterization of the biosynthesis and integration of the Photosystem II reaction centers in the thylakoid membrane of Chlamydomonas reinhardtii. EMBO J 3: 701-706
Pubmed: Author and Title
Google Scholar: Author Only Title Only Author and Title

Delosme R, Olive J, Wollman FA (1996) Changes in light energy distribution upon state transitions: An in vivo photoacoustic study of the wild type and photosynthesis mutants from Chlamydomonas reinhardtii. Biochimica Et Biophysica Acta-Bioenergetics 1273: 150-158

Pubmed: Author and Title
Google Scholar: Author Only Title Only Author and Title

Depege N, Bellafiore S, Rochaix JD (2003) Role of chloroplast protein kinase Stt7 in LHCII phosphorylation and state transition in Chlamydomonas. Science 299: 1572-1575
Pubmed: Author and Title
Google Scholar: Author Only Title Only Author and Title

Devitry C, Wollman FA (1988) Changes in Phosphorylation of Thylakoid Membrane-Proteins in Light-Harvesting Complex Mutants from Chlamydomonas-Reinhardtii. Biochimica Et Biophysica Acta 933: 444-449
Pubmed: Author and Title
Google Scholar: Author Only Title Only Author and Title

Douchi D, Qu Y, Longoni P, Legendre-Lefebvre L, Johnson X, Schmitz-Linneweber C, Goldschmidt-Clermont M (2016) A Nucleus-Encoded Chloroplast Phosphoprotein Governs Expression of the Photosystem I Subunit PsaC in Chlamydomonas reinhardtii. Plant Cell 28: 1182-1199
Pubmed: Author and Title
Google Scholar: Author Only Title Only Author and Title

Drop B, Webber-Birungi M, Fusetti F, Kouril R, Redding KE, Boekema EJ, Croce R (2011) Photosystem I of Chlamydomonas reinhardtii contains nine light-harvesting complexes (Lhca) located on one side of the core. J Biol Chem 286: 44878-44887
Pubmed: Author and Title
Google Scholar: Author Only Title Only Author and Title

Drop B, Yadav KNS, Boekema EJ, Croce R (2014) Consequences of state transitions on the structural and functional organization of photosystem I in the green alga Chlamydomonas reinhardtii. Plant J 78: 181-191
Pubmed: Author and Title
Google Scholar: Author Only Title Only Author and Title

Dumas L, Zito F, Blangy S, Auroy P, Johnson X, Peltier G, Alric J (2017) A stromal region of cytochrome b6f subunit IV is involved in the activation of the Stt7 kinase in Chlamydomonas. Proc Natl Acad Sci U S A 114: 12063-12068
Pubmed: Author and Title
Google Scholar: Author Only Title Only Author and Title

Eberhard S, Finazzi G, Wollman FA (2008) The dynamics of photosynthesis. Annu Rev Genet 42: 463-515
Pubmed: Author and Title
Google Scholar: Author Only Title Only Author and Title

Elrad D, Grossman AR (2004) A genome's-eye view of the light-harvesting polypeptides of Chlamydomonas reinhardtii. Curr Genet 45: 61-75
Pubmed: Author and Title
Google Scholar: Author Only Title Only Author and Title

Emanuelsson O, Nielsen H, von Heijne G (1999) ChloroP, a neural network-based method for predicting chloroplast transit peptides and their cleavage sites. Protein Sci 8: 978-984
Pubmed: Author and Title
Google Scholar: Author Only Title Only Author and Title

Ferrante P, Ballottari M, Bonente G, Giuliano G, Bassi R (2012) LHCBM1 and LHCBM2/7 polypeptides, components of major LHCII complex, have distinct functional roles in photosynthetic antenna system of Chlamydomonas reinhardtii. J Biol Chem 287: 16276-16288
Pubmed: Author and Title
Google Scholar: Author Only Title Only Author and Title

Ferrante P, Ballottari M, Bonente G, Giuliano G, Bassi R (2012) LHCBM1 and LHCBM2/7 polypeptides, components of major LHCII complex, have distinct functional roles in photosynthetic antenna system of Chlamydomonas reinhardtii. The Journal of biological chemistry 287: 16276-16288
Pubmed: Author and Title
Google Scholar: Author Only Title Only Author and Title

Finazzi G, Rappaport F, Furia A, Fleischmann M, Rochaix JD, Zito F, Forti G (2002) Involvement of state transitions in the switch between linear and cyclic electron flow in Chlamydomonas reinhardtii. EMBO Rep 3: 280-285
Pubmed: Author and Title
Google Scholar: Author Only Title Only Author and Title

Fleischmann MM, Ravanel S, Delosme R, Olive J, Zito F, Wollman FA, Rochaix JD (1999) Isolation and characterization of photoautotrophic mutants of Chlamydomonas reinhardtii deficient in state transition. J Biol Chem 274: 30987-30994
Pubmed: Author and Title
Google Scholar: Author Only Title Only Author and Title

Galka P, Santabarbara S, Khuong TT, Degand H, Morsomme P, Jennings RC, Boekema EJ, Caffarri S (2012) Functional analyses of the plant photosystem I-light-harvesting complex II supercomplex reveal that light-harvesting complex II loosely bound to photosystem II is a very efficient antenna for photosystem I in state II. Plant Cell 24: 2963-2978
Pubmed: Author and Title
Google Scholar: Author Only Title Only Author and Title

Gibson DG, Young L, Chuang RY, Venter JC, Hutchison CA, 3rd, Smith HO (2009) Enzymatic assembly of DNA molecules up to several hundred kilobases. Nat Methods 6: 343-345
Pubmed: Author and Title
Google Scholar: Author Only Title Only Author and Title

Girolomoni L, Ferrante P, Berteotti S, Giuliano G, Bassi R, Ballottari M (2017) The function of LHCBM4/6/8 antenna proteins in Chlamydomonas reinhardtii. J Exp Bot 68: 627-641
Pubmed: Author and Title
Google Scholar: Author Only Title Only Author and Title

Goldschmidt-Clermont M, Bassi R (2015) Sharing light between two photosystems: mechanism of state transitions. Curr Opin Plant Biol 25: 71-78
Pubmed: Author and Title
Google Scholar: Author Only Title Only Author and Title

Gonzalez-Ballester D, de Montaigu A, Galvan A, Fernandez E (2005) Restriction enzyme site-directed amplification PCR: a tool to identify regions flanking a marker DNA. Anal Biochem 340: 330-335
Pubmed: Author and Title
Google Scholar: Author Only Title Only Author and Title

Grewe S, Ballottari M, Alcocer M, D'Andrea C, Blifernez-Klassen O, Hankamer B, Mussgnug JH, Bassi R, Kruse O (2014) Light-Harvesting Complex Protein LHCBM9 Is Critical for Photosystem II Activity and Hydrogen Production in Chlamydomonas reinhardtii. Plant Cell 26: 1598-1611
Pubmed: Author and Title
Google Scholar: Author Only Title Only Author and Title

Hamel P, Olive J, Pierre Y, Wollman FA, de Vitry C (2000) A new subunit of cytochrome b6f complex undergoes reversible phosphorylation upon state transition. J Biol Chem 275: 17072-17079
Pubmed: Author and Title
Google Scholar: Author Only Title Only Author and Title

Hodges M, Barber J (1983) State 1-State 2 Transitions in a Unicellular Green Algae : Analysis of In Vivo Chlorophyll Fluorescence Induction Curves in the Presence of 3-(3,4-Dichlorophenyl)-1, 1-dimethylurea (DCMU). Plant Physiol 72: 1119-1122
Pubmed: Author and Title
Google Scholar: Author Only Title Only Author and Title

Houille-Vernes L, Rappaport F, Wollman FA, Alric J, Johnson X (2011) Plastid terminal oxidase 2 (PTOX2) is the major oxidase involved in chlororespiration in Chlamydomonas. Proc Natl Acad Sci U S A 108: 20820-20825
Pubmed: Author and Title
Google Scholar: Author Only Title Only Author and Title

Iwai M, Roth MS, Niyogi KK (2018) Subdiffraction-resolution live-cell imaging for visualizing thylakoid membranes. Plant J
Pubmed: Author and Title
Google Scholar: Author Only Title Only Author and Title

Iwai M, Takizawa K, Tokutsu R, Okamuro A, Takahashi Y, Minagawa J (2010) Isolation of the elusive supercomplex that drives cyclic electron flow in photosynthesis. Nature 464: 1210-1213
Pubmed: Author and Title
Google Scholar: Author Only Title Only Author and Title

Johnson X, Vandystadt G, Bujaldon S, Wollman FA, Dubois R, Roussel P, Alric J, Beal D (2009) A new setup for in vivo fluorescence imaging of photosynthetic activity. Photosynth Res 102: 85-93
Pubmed: Author and Title
Google Scholar: Author Only Title Only Author and Title

Kinoshita E, Kinoshita-Kikuta E, Koike T (2009) Separation and detection of large phosphoproteins using Phos-tag SDS-PAGE. Nat Protoc 4: 1513-1521
Pubmed: Author and Title
Google Scholar: Author Only Title Only Author and Title

Kubota-Kawai H, Burton-Smith RN, Tokutsu R, Song C, Akimoto S, Yokono M, Ueno Y, Kim E, Watanabe A, Murata K, Minagawa J (2019) Ten antenna proteins are associated with the core in the supramolecular organization of the photosystem I supercomplex in Chlamydomonas reinhardtii. J Biol Chem
Pubmed: Author and Title
Google Scholar: Author Only Title Only Author and Title

Lemeille S, Turkina MV, Vener AV, Rochaix JD (2010) Stt7-dependent phosphorylation during state transitions in the green alga Chlamydomonas reinhardtii. Mol Cell Proteomics 9: 1281-1295
Pubmed: Author and Title
Google Scholar: Author Only Title Only Author and Title

Lemeille S, Turkina MV, Vener AV, Rochaix JD (2010) Stt7-dependent phosphorylation during state transitions in the green alga Chlamydomonas reinhardtii. Molecular & cellular proteomics : MCP 9: 1281-1295
Pubmed: Author and Title
Google Scholar: Author Only Title Only Author and Title

Li X, Zhang R, Patena W, Gang SS, Blum SR, Ivanova N, Yue R, Robertson JM, Lefebvre PA, Fitz-Gibbon ST, Grossman AR, Jonikas MC (2016) An Indexed, Mapped Mutant Library Enables Reverse Genetics Studies of Biological Processes in Chlamydomonas reinhardtii. Plant Cell 28: 367-387
Pubmed: Author and Title
Google Scholar: Author Only Title Only Author and Title

Liu X, Chai J, Ou X, Li M, Liu Z (2018) Structural insights into substrate selectivity, catalytic mechanism and redox regulation of rice photosystem II core phosphatase. Mol Plant
Pubmed: Author and Title
Google Scholar: Author Only Title Only Author and Title

Longoni P, Douchi D, Cariti F, Fucile G, Goldschmidt-Clermont M (2015) Phosphorylation of the Light-Harvesting Complex II Isoform Lhcb2 Is Central to State Transitions. Plant Physiol 169: 2874-2883
Pubmed: Author and Title
Google Scholar: Author Only Title Only Author and Title

Longoni P, Samol I, Goldschmidt-Clermont M (2019) The Kinase STATE TRANSITION 8 Phosphorylates Light Harvesting Complex II and Contributes to Light Acclimation in Arabidopsis thaliana. Front Plant Sci 10: 1156
Pubmed: Author and Title
Google Scholar: Author Only Title Only Author and Title

Mazor Y, Borovikova A, Nelson N (2015) The structure of plant photosystem I super-complex at 2.8 A resolution. Elife 4: e07433
Pubmed: Author and Title
Google Scholar: Author Only Title Only Author and Title

Merchant SS, Prochnik SE, Vallon O, Harris EH, Karpowicz SJ, Witman GB, Terry A, Salamov A, Fritz-Laylin LK, Marechal-Drouard L, Marshall WF, Qu LH, Nelson DR, Sanderfoot AA, Spalding MH, Kapitonov VV, Ren Q, Ferris P, Lindquist E, Shapiro H, Lucas SM, Grimwood J, Schmutz J, Cardol P, Cerutti H, Chanfreau G, Chen CL, Cognat V, Croft MT, Dent R, Dutcher S, Fernandez E, Fukuzawa H, Gonzalez-Ballester D, Gonzalez-Halphen D, Hallmann A, Hanikenne M, Hippler M, Inwood W, Jabbari K, Kalanon M, Kuras R, Lefebvre PA, Lemaire SD, Lobanov AV, Lohr M, Manuell A, Meier I, Mets L, Mittag M, Mittelmeier T, Moroney JV, Moseley J, Napoli C, Nedelcu AM, Niyogi K, Novoselov SV, Paulsen IT, Pazour G, Purton S, Ral JP, Riano-Pachon DM, Riekhof W, Rymarquis L, Schroda M, Stern D, Umen J, Willows R, Wilson N, Zimmer SL, Allmer J, Balk J, Bisova K, Chen CJ, Elias M, Gendler K, Hauser C, Lamb MR, Ledford H, Long JC, Minagawa J, Page MD, Pan J, Pootakham W, Roje S, Rose A, Stahlberg E, Terauchi AM, Yang P, Ball S, Bowler C, Dieckmann CL, Gladyshev VN, Green P, Jorgensen R, Mayfield S, Mueller-Roeber B, Rajamani S, Sayre RT, Brokstein P, Dubchak I, Goodstein D, Hornick L, Huang YW, Jhaveri J, Luo Y, Martinez D, Ngau WC, Otillar B, Poliakov A, Porter A, Szajkowski L, Werner G, Zhou K, Grigoriev IV, Rokhsar DS, Grossman AR (2007) The Chlamydomonas genome reveals the evolution of key animal and plant functions. Science 318: 245-250
Pubmed: Author and Title
Google Scholar: Author Only Title Only Author and Title

Minagawa J, Takahashi Y (2004) Structure, function and assembly of Photosystem II and its light-harvesting proteins. Photosynth Res 82: 241-263
Pubmed: Author and Title
Google Scholar: Author Only Title Only Author and Title

Nagy G, Unnep R, Zsiros O, Tokutsu R, Takizawa K, Porcar L, Moyet L, Petroutsos D, Garab G, Finazzi G, Minagawa J (2014) Chloroplast remodeling during state transitions in Chlamydomonas reinhardtii as revealed by noninvasive techniques in vivo. Proc Natl Acad Sci U S A 111: 5042-5047
Pubmed: Author and Title
Google Scholar: Author Only Title Only Author and Title

Natali A, Croce R (2015) Characterization of the major light-harvesting complexes (LHCBM) of the green alga Chlamydomonas reinhardtii. PLoS One 10: e0119211
Pubmed: Author and Title
Google Scholar: Author Only Title Only Author and Title

Nawrocki WJ, Santabarbara S, Mosebach L, Wollman FA, Rappaport F (2016) State transitions redistribute rather than dissipate energy between the two photosystems in Chlamydomonas. Nat Plants 2: 16031
Pubmed: Author and Title
Google Scholar: Author Only Title Only Author and Title

Ozawa SI, Bald T, Onishi T, Xue H, Matsumura T, Kubo R, Takahashi H, Hippler M, Takahashi Y (2018) Configuration of Ten Light-Harvesting Chlorophyll a/b Complex I Subunits in Chlamydomonas reinhardtii Photosystem I. Plant Physiol 178: 583-595
Pubmed: Author and Title
Google Scholar: Author Only Title Only Author and Title

Pan X, Ma J, Su X, Cao P, Chang W, Liu Z, Zhang X, Li M (2018) Structure of the maize photosystem I supercomplex with light-harvesting complexes I and II. Science 360: 1109-1113
Pubmed: Author and Title
Google Scholar: Author Only Title Only Author and Title

Pietrzykowska M, Suorsa M, Semchonok DA, Tikkanen M, Boekema EJ, Aro EM, Jansson S (2014) The Light-Harvesting Chlorophyll a/b Binding Proteins Lhcb1 and Lhcb2 Play Complementary Roles during State Transitions in Arabidopsis. Plant Cell 26: 3646-3660

Pubmed: Author and Title
Google Scholar: Author Only Title Only Author and Title

Pribil M, Pesaresi P, Hertle A, Barbato R, Leister D (2010) Role of plastid protein phosphatase TAP38 in LHCII dephosphorylation and thylakoid electron flow. PLoS Biol 8: e1000288
Pubmed: Author and Title
Google Scholar: Author Only Title Only Author and Title

Puthiyaveetil S, Woodiwiss T, Knoerdel R, Zia A, Wood M, Hoehner R, Kirchhoff H (2014) Significance of the photosystem II core phosphatase PBCP for plant viability and protein repair in thylakoid membranes. Plant Cell Physiol 55: 1245-1254
Pubmed: Author and Title
Google Scholar: Author Only Title Only Author and Title

Ramundo S, Rahire M, Schaad O, Rochaix JD (2013) Repression of essential chloroplast genes reveals new signaling pathways and regulatory feedback loops in chlamydomonas. Plant Cell 25: 167-186
Pubmed: Author and Title
Google Scholar: Author Only Title Only Author and Title

Rantala M, Lehtimaki N, Aro EM, Suorsa M (2016) Downregulation of TAP38/PPH1 enables LHCII hyperphosphorylation in Arabidopsis mutant lacking LHCII docking site in PSI. FEBS Lett 590: 787-794
Pubmed: Author and Title
Google Scholar: Author Only Title Only Author and Title

Reiland S, Finazzi G, Endler A, Willig A, Baerenfaller K, Grossmann J, Gerrits B, Rutishauser D, Gruissem W, Rochaix JD, Baginsky S (2011) Comparative phosphoproteome profiling reveals a function of the STN8 kinase in fine-tuning of cyclic electron flow (CEF). Proceedings of the National Academy of Sciences of the United States of America 108: 12955-12960
Pubmed: Author and Title
Google Scholar: Author Only Title Only Author and Title

Rochaix JD (2014) Regulation and dynamics of the light-harvesting system. Annu Rev Plant Biol 65: 287-309
Pubmed: Author and Title
Google Scholar: Author Only Title Only Author and Title

Rochaix JD, Lemeille S, Shapiguzov A, Samol I, Fucile G, Willig A, Goldschmidt-Clermont M (2012) Protein kinases and phosphatases involved in the acclimation of the photosynthetic apparatus to a changing light environment. Philos Trans R Soc Lond B Biol Sci 367: 3466-3474
Pubmed: Author and Title
Google Scholar: Author Only Title Only Author and Title

Samol I, Shapiguzov A, Ingelsson B, Fucile G, Crevecoeur M, Vener AV, Rochaix JD, Goldschmidt-Clermont M (2012) Identification of a Photosystem II Phosphatase Involved in Light Acclimation in Arabidopsis. The Plant cell
Pubmed: Author and Title
Google Scholar: Author Only Title Only Author and Title

Samol I, Shapiguzov A, Ingelsson B, Fucile G, Crevecoeur M, Vener AV, Rochaix JD, Goldschmidt-Clermont M (2012) Identification of a photosystem II phosphatase involved in light acclimation in Arabidopsis. Plant Cell 24: 2596-2609
Pubmed: Author and Title
Google Scholar: Author Only Title Only Author and Title

Shapiguzov A, Ingelsson B, Samol I, Andres C, Kessler F, Rochaix JD, Vener AV, Goldschmidt-Clermont M (2010) The PPH1 phosphatase is specifically involved in LHCII dephosphorylation and state transitions in Arabidopsis. Proc Natl Acad Sci U S A 107: 4782-4787
Pubmed: Author and Title
Google Scholar: Author Only Title Only Author and Title

Shimogawara K, Fujiwara S, Grossman A, Usuda H (1998) High-efficiency transformation of Chlamydomonas reinhardtii by electroporation. Genetics 148: 1821-1828
Pubmed: Author and Title
Google Scholar: Author Only Title Only Author and Title

Sizova I, Fuhrmann M, Hegemann P (2001) A Streptomyces rimosus aphVIII gene coding for a new type phosphotransferase provides stable antibiotic resistance to Chlamydomonas reinhardtii. Gene 277: 221-229
Pubmed: Author and Title
Google Scholar: Author Only Title Only Author and Title

Stauber EJ, Fink A, Markert C, Kruse O, Johanningmeier U, Hippler M (2003) Proteomics of Chlamydomonas reinhardtii light-harvesting proteins. Eukaryot Cell 2: 978-994
Pubmed: Author and Title
Google Scholar: Author Only Title Only Author and Title

Steinbeck J, Ross IL, Rothnagel R, Gabelein P, Schulze S, Giles N, Ali R, Drysdale R, Sierecki E, Gambin Y, Stahlberg H, Takahashi Y, Hippler M, Hankamer B (2018) Structure of a PSI-LHCI-cyt b6f supercomplex in Chlamydomonas reinhardtii promoting cyclic electron flow under anaerobic conditions. Proc Natl Acad Sci U S A 115: 10517-10522
Pubmed: Author and Title
Google Scholar: Author Only Title Only Author and Title

Takahashi H, Clowez S, Wollman FA, Vallon O, Rappaport F (2013) Cyclic electron flow is redox-controlled but independent of state transition. Nat Commun 4: 1954
Pubmed: Author and Title
Google Scholar: Author Only Title Only Author and Title

Takahashi H, Iwai M, Takahashi Y, Minagawa J (2006) Identification of the mobile light-harvesting complex II polypeptides for state transitions in Chlamydomonas reinhardtii. Proceedings of the National Academy of Sciences of the United States of America 103: 477-482
Pubmed: Author and Title
Google Scholar: Author Only Title Only Author and Title

Takahashi H, Iwai M, Takahashi Y, Minagawa J (2006) Identification of the mobile light-harvesting complex II polypeptides for state transitions in Chlamydomonas reinhardtii. Proc Natl Acad Sci U S A 103: 477-482
Pubmed: Author and Title
Google Scholar: Author Only Title Only Author and Title

Takahashi H, Okamuro A, Minagawa J, Takahashi Y (2014) Biochemical characterization of photosystem I-associated light-harvesting complexes I and II isolated from state 2 cells of Chlamydomonas reinhardtii. Plant Cell Physiol 55: 1437-1449
Pubmed: Author and Title
Google Scholar: Author Only Title Only Author and Title

Takahashi H, Schmollinger S, Lee JH, Schroda M, Rappaport F, Wollman FA, Vallon O (2016) The PETO protein interacts with other effectors of cyclic electron flow in Chlamydomonas. Mol Plant
Pubmed: Author and Title
Google Scholar: Author Only Title Only Author and Title

Takahashi Y, Yasui TA, Stauber EJ, Hippler M (2004) Comparison of the subunit compositions of the PSI-LHCI supercomplex and the LHCI in the green alga Chlamydomonas reinhardtii. Biochemistry 43: 7816-7823
Pubmed: Author and Title
Google Scholar: Author Only Title Only Author and Title

Tapie P, Choquet Y, Breton J, Delepelaire P, Wollman FA (1984) Orientation of photosystem-I pigments. Investigation by low-temperature linear dichroism and polarized fluorescence emission. Biochimica et Biophysica Acta (BBA) - Bioenergetics 767: 57-69
Pubmed: Author and Title
Google Scholar: Author Only Title Only Author and Title

Tardif M, Atteia A, Specht M, Cogne G, Rolland N, Brugiere S, Hippler M, Ferro M, Bruley C, Peltier G, Vallon O, Cournac L (2012) PredAlgo: a new subcellular localization prediction tool dedicated to green algae. Mol Biol Evol 29: 3625-3639
Pubmed: Author and Title
Google Scholar: Author Only Title Only Author and Title

Tokutsu R, Iwai M, Minagawa J (2009) CP29, a monomeric light-harvesting complex II protein, is essential for state transitions in Chlamydomonas reinhardtii. J Biol Chem 284: 7777-7782
Pubmed: Author and Title
Google Scholar: Author Only Title Only Author and Title

Tolleter D, Ghysels B, Alric J, Petroutsos D, Tolstygina I, Krawietz D, Happe T, Auroy P, Adriano JM, Beyly A, Cuine S, Plet J, Reiter IM, Genty B, Cournac L, Hippler M, Peltier G (2011) Control of hydrogen photoproduction by the proton gradient generated by cyclic electron flow in Chlamydomonas reinhardtii. Plant Cell 23: 2619-2630
Pubmed: Author and Title
Google Scholar: Author Only Title Only Author and Title

Turkina MV, Kargul J, Blanco-Rivero A, Villarejo A, Barber J, Vener AV (2006) Environmentally modulated phosphoproteome of photosynthetic membranes in the green alga Chlamydomonas reinhardtii. Molecular & cellular proteomics : MCP 5: 1412-1425
Pubmed: Author and Title
Google Scholar: Author Only Title Only Author and Title

Unlu C, Drop B, Croce R, van Amerongen H (2014) State transitions in Chlamydomonas reinhardtii strongly modulate the functional size of photosystem II but not of photosystem I. Proc Natl Acad Sci U S A 111: 3460-3465
Pubmed: Author and Title
Google Scholar: Author Only Title Only Author and Title

Vainonen JP, Hansson M, Vener AV (2005) STN8 protein kinase in Arabidopsis thaliana is specific in phosphorylation of photosystem II core proteins. J Biol Chem 280: 33679-33686
Pubmed: Author and Title
Google Scholar: Author Only Title Only Author and Title

Vener AV, van Kan PJ, Rich PR, Ohad I, Andersson B (1997) Plastoquinol at the quinol oxidation site of reduced cytochrome bf mediates signal transduction between light and protein phosphorylation: thylakoid protein kinase deactivation by a single-turnover flash. Proc Natl Acad Sci U S A 94: 1585-1590
Pubmed: Author and Title
Google Scholar: Author Only Title Only Author and Title

Wei X, Guo J, Li M, Liu Z (2015) Structural Mechanism Underlying the Specific Recognition between the Arabidopsis State-Transition

Phosphatase TAP38/PPH1 and Phosphorylated Light-Harvesting Complex Protein Lhcb1. Plant Cell 27: 1113-1127
Pubmed: Author and Title
Google Scholar: Author Only Title Only Author and Title

Willig A, Shapiguzov A, Goldschmidt-Clermont M, Rochaix JD (2011) The Phosphorylation Status of the Chloroplast Protein Kinase STN7 of Arabidopsis Affects Its Turnover. Plant physiology 157: 2102-2107
Pubmed: Author and Title
Google Scholar: Author Only Title Only Author and Title

Wlodarczyk LM, Snellenburg JJ, Ihalainen JA, van Grondelle R, van Stokkum IH, Dekker JP (2015) Functional rearrangement of the light-harvesting antenna upon state transitions in a green alga. Biophys J 108: 261-271
Pubmed: Author and Title
Google Scholar: Author Only Title Only Author and Title

Wollman FA, Delepelaire P (1984) Correlation between changes in light energy distribution and changes in thylakoid membrane polypeptide phosphorylation in Chlamydomonas reinhardtii. J Cell Biol 98: 1-7
Pubmed: Author and Title
Google Scholar: Author Only Title Only Author and Title

Yadav KN, Semchonok DA, Nosek L, Kouril R, Fucile G, Boekema EJ, Eichacker LA (2017) Supercomplexes of plant photosystem I with cytochrome b6f, light-harvesting complex II and NDH. Biochim Biophys Acta 1858: 12-20
Pubmed: Author and Title
Google Scholar: Author Only Title Only Author and Title

Yamori W, Shikanai T (2016) Physiological Functions of Cyclic Electron Transport Around Photosystem I in Sustaining Photosynthesis and Plant Growth. Annu Rev Plant Biol 67: 81-106
Pubmed: Author and Title
Google Scholar: Author Only Title Only Author and Title

Zito F, Finazzi G, Delosme R, Nitschke W, Picot D, Wollman FA (1999) The Qo site of cytochrome b_6f complexes controls the activation of the LHCII kinase. The EMBO Journal 18: 2961-2969
Pubmed: Author and Title
Google Scholar: Author Only Title Only Author and Title